Multiple Temporal and Object-Based Strategies Across Learning for a Selective Detection Task in Mice

Abstract

Goal-directed behavior paradigms inevitably involve temporal processes, such as anticipation, expectation, timing, waiting, and withholding. And yet, amongst the vast use of object-based task paradigms, characterizations of temporal features are often neglected. Here, we longitudinally analyzed mice from naïve to expert performance in a somatosensory selective detection task. In addition to tracking standard measures from signal detection theory, we also characterized learning of temporal features. We find that mice transition from general sampling strategies to stimulus detection and stimulus discrimination. During these transitions, mice learn to wait as they anticipate an expected stimulus presentation and to time their response after a stimulus presentation. By establishing and implementing standardized measures, we show that the development of waiting and timing in the task overlaps with learning of stimulus detection and discrimination. We also investigated sex differences in temporal and object-based trajectories of learning, finding that males learn strategies idiosyncratically and that females learn strategies more sequentially and stereotypically. Overall, our findings emphasize multiple temporal strategies in learning for an object-based task and highlight the importance of considering diverse temporal and object-based features when characterizing behavioral and neuronal aspects of learning.

Introduction

All behavior operates within a temporal structure. Moreover, temporal processes, such as anticipation, expectation, timing, waiting, and withholding, significantly impact performance on object-based tasks (Cravo et al., 2017; Grabenhorst et al., 2019; Guo et al., 2014). And yet, object-based versus temporal processes in behavioral tasks are often investigated in isolation from each other (Buhusi & Meck, 2005; Dent & Neill, 2012; Murakami et al., 2017; Narayanan et al., 2012; Paton & Buonomano, 2018; Richter & von Kortzfleisch, 2020; Womelsdorf & Fries, 2007). Understanding temporal processes may be particularly important in the study of neuropsychiatric disease. In disorders such as autism spectrum disorder (ASD), attention deficit hyperactivity disorder (ADHD), learning disorders, and schizophrenia, greater disparities are observed across temporal (interval estimation, perception) compared to object-based (frequency, localization, categorization, orientation, spatial) features (Bayard et al., 2020; Carroll et al., 2009; Eden et al., 1995; Lee et al., 2009; Meilleur et al., 2020; Pardey et al., 2009; Rubia et al., 2009; Toplak et al., 2006). For example, in a study of ADHD versus control children, deficits were not found in reporting visual stimulus detection. Rather, deficits were found in fixation and countermanding: ADHD children tended to demonstrate larger and more frequent breaks in visual fixation and increased errors, faster responses to go signals, and slower responses to stop signals (Hanisch et al., 2006).

For training in any object-based task, learning must occur for both object-based and temporal features. Object-based paradigms such as detection (Huber et al., 2012), discrimination (Erlich et al., 2011; Pai et al., 2011; Rudebeck & Murray, 2008; Song et al., 2020), categorization (Freedman et al., 2003; Reinert et al., 2021), and sequencing (Jin & Costa, 2010; Smits-Bandstra & De Nil, 2007) require learning of temporal features such as anticipation (Chen et al., 2017; McClure et al., 2003), evidence accumulation (Churchland et al., 2011; Erlich et al., 2015; Roitman & Shadlen, 2002), impulse control (Peterson et al., 1999; Robbins & Dalley, 2017; Winstanley et al., 2004), reward discounting (Kable & Glimcher, 2007; Mar et al., 2011; Mobini et al., 2002), starting and stopping (Bari & Robbins, 2013; Hanisch et al., 2006), and temporal uncertainty (Daw et al., 2005; Fiorillo et al., 2003; Lawson et al., 2021; Mendonça et al., 2020). Moreover, learning may not track along a single continuum from naïve to expert but may involve transitions between intermediate strategies. For instance, just as optimal temporal strategies are learned, such as fast reaction times for a detection paradigm (Baunez & Robbins, 1997, 1999), suboptimal strategies must be unlearned, such as fast reaction times for a waiting paradigm (Narayanan et al., 2006; Reyes et al., 2020).

This investigation explores the relationship between learning of temporal and object-based features from naïve to expert performance for a selective sensory detection task in mice. Along with traditional measures of sensory detection, we address two specific temporal processes, waiting and timing, which are not typically studied in object-based tasks (Komiyama et al., 2010; McBurney-Lin et al., 2020; Ruff & Cohen, 2019; Xiong et al., 2015; Yang et al., 2019) and vice versa (Bakhurin et al., 2017; Droit-Volet et al., 2007; Kawai et al., 2015; Lak et al., 2014; Namboodiri et al., 2015; Shuler & Bear, 2006). 1) *Sampling versus Waiting*: naïve behavior involves high sampling and low waiting before stimulus presentation (Dickinson & Balleine, 1994; O'Doherty et al., 2003; Schoenbaum & Roesch, 2005). The null hypothesis predicts that sampling behavior and waiting behavior do not change while learning sensory detection and discrimination. An alternative hypothesis predicts that sampling behavior decreases and waiting behavior increases as performance improves. 2) *Reacting versus Timing*: due to response sampling, post-stimulus reaction times in naïve behavior are long and broadly distributed (Laubach et al., 2000; van Maanen et al., 2012). A reactive hypothesis predicts that with learning of sensory detection, reaction times decrease towards a biophysical response limit (Duan et al., 2015; Romo & Schultz, 1990; Schultz et al., 1993). An alternative timing hypothesis predicts the convergence of reaction times to a task-specific optimal response latency.

Additional questions addressed in this study focus on learning trajectories. During learning of a sensory detection task, do mice transition in stages of intermediate strategies? Do mice learn temporal features before, after, or in tandem with object-based features? Are there sex-specific transitions, intermediates, or orders of learning? By addressing these questions, we strive to better understand the temporal and object-based features that mice learn during different phases of training. With this knowledge, we will be better equipped to determine the neural mechanisms underlying temporal and object-based learning.

Here, we use temporal and object-based measures to track learning for a whisker-based selective detection task, with target or distractor whisker stimuli presented in individual trials. We find transitions from suboptimal *sampling* to optimal *waiting* before a stimulus and to optimal *timing* after a stimulus. Additionally, we identify learning trajectories in which temporal and object-based feature learning overlap. Lastly, we identify sex-based differences in the order of learning, transition magnitudes, and intermediate strategies. These findings emphasize the importance of tracking multiple measures through learning, for a more comprehensive understanding of both learning behavior and its neural mechanisms.

Results

Learning strategies for a selective detection task. We used an object-based selective detection paradigm to investigate concurrent temporal strategies across learning in mice (Figure 1A). In this task, water-restricted mice learn to selectively respond to target paddle deflections in one whisker field (hit, rewarded with water delivery) and ignore distractor paddle deflections in the opposite whisker field (correct rejection). We impose a variable intertrial interval (ITI) between 5.5 and 9.5 s, chosen to reduce spontaneous sampling before stimulus presentation. Target and distractor stimuli were presented probabilistically; the correct rejection of a distractor stimulus initiated the next trial, a target trial preceded by a shortened 0.2 to 1.9 s ITI. Overall, mice must wait (withhold licking) across a duration of minimum 5.5 s (ITI_{min}) to maximum 14.6 s (ITI_{max}) to be presented with a target stimulus and opportunity for reward (Figure 1B). Prepotent responses during the ITI were defined as spontaneous sampling (Spont) and resulted in a resetting of the ITI. Additionally, we implemented a minimum 200 ms lockout period after a stimulus presentation. Therefore, mice were required to respond on target trials after this lockout period to trigger a reward. In our previous studies of this task, expert performance was determined solely by target and distractor stimulus discrimination. Given the temporal structures described above, here, we additionally test a waiting strategy by exploring interlick interval (ILI) distributions for all lick responses and we test a timing strategy by exploring reaction time (RT) distributions for responses to stimuli (Figure 1C).

In this study we present longitudinal data from 52 mice. An increase in discrimination (separation of hit rate and false alarm rate) across terciles of training sessions indicated a learning trajectory from naïve to expert

performance (Figure 1D, unbalanced one-way $ANOVA_{d'TercDiscrim}$ $F(2,573)=167.49$, $p<0.0005$). Across the same training sessions, we also observed a decrease in criterion bias, indicating an increased tendency to respond across target and distractor trials (Figure 1E, unbalanced one-way $ANOVA_{TercCriterion}$ $F(2,573)=59.47$, $p<0.0005$).

Transition in waiting behavior. We next investigated the temporal strategy of sampling versus waiting across learning. We tested the hypothesis that, due to the variable ITI imposition, suboptimal sampling behavior (ILI shorter than ITI_{min}) decreases while optimal waiting behavior (ILI longer than ITI_{min} and shorter than ITI_{max}) increases across learning. These analyses address a temporal phenotype before target stimulus presentation. The null hypothesis is that mice do not change their sampling and waiting behavior across learning (Figure 2A). Alternatively, we expect a divergence in sampling and waiting behavior across learning (Figure 2B), indicating an improvement in waiting.

We identified sampling and waiting by defining a sampling criterion (spontaneous responding within the minimum ITI before a stimulus) and a waiting criterion (responding after successfully waiting for a stimulus). We investigated sampling versus waiting behavior across sessions binned as early, middle, and late tercile stages of training (Figure 2C-E). For 'all responses' (Figure 2C, including sampling and waiting), we note that early and late tercile counts of all lick responses are not significantly different; however, responses increased significantly from early to middle terciles (Figure 2C, unbalanced one-way $ANOVA_{TercILICount}$ $F(2,573)=4.45$, $p=0.0121$). Sampling responses ($ILI<ITI_{min}$) significantly decreased from middle to late terciles with a nonsignificant increase between early and middle terciles (Figure 2D, unbalanced one-way $ANOVA_{TercSampCount}$ $F(2,573)=3.72$, $p=0.0249$). Waiting responses ($ITI_{min}<ILI<ITI_{max}$) increased significantly from early to middle terciles and remained elevated, with a nonsignificant increase from middle to late terciles (Figure 2E, unbalanced one-way $ANOVA_{TercWaitCount}$ $F(2,573)=22.20$, $p<0.0005$). Thus, all response distributions increased from early to middle terciles; sampling responses then decreased while waiting responses remained high from middle to late terciles.

To quantify sampling and waiting distributions, we calculated the area under the sampling curve and the area under the waiting curve and normalized by the total area under the 'all response' curve. This analysis generated sampling % AUC values and waiting % AUC values (Figure 2F). Sampling % AUC decreased significantly across all terciles (unbalanced one-way $ANOVA_{TercSamp\%AUC}$ $F(2,573)=24.19$, $p<0.0005$) and waiting % AUC increased significantly across all terciles (unbalanced one-way $ANOVA_{TercWait\%AUC}$ $F(2,573)=42.15$, $p<0.0005$). We also quantified waiting strategies per mouse by plotting % AUC for each session across learning and determining the slopes of a linear fit (Figure 2F). We found that sampling % AUC decreased significantly across sessions per mouse (one sample t-test $\mu_{mSamp\%AUC}=-2.003\pm0.386$, $p<0.0005$, $n=52$ mice) and that waiting % AUC increased significantly across sessions per mouse (one sample t-test $\mu_{mWait\%AUC}=2.248\pm0.353$, $p<0.0005$, $n=52$ mice). Overall, these analyses demonstrate robust changes in prestimulus behavior, with progressive decreases in sampling and increases in waiting.

As waiting behavior improves, we would expect the ILI distribution to shift towards longer intervals (Figure 2G). We investigated the ILI cumulative distribution function (CDF) and found that it shifted rightward towards longer ILIs (plotted for all sessions across mice, averaged terciles for all mice, and averaged terciles across mice, Figure 2H-J, respectively). In addition to simply considering sessions (by terciles) in training, we also plotted these CDFs according to target-distractor stimulus discrimination performance, for naïve ($d'<0.8$), intermediate ($0.8<d'<1.2$), and expert ($d'>1.2$) behavior. Interestingly, we found that CDF curves during naïve and intermediate performance were similar, and markedly different from CDF curves during expert performance (Figure 2K). We quantified the shift in CDF curves by the median ILI across terciles and across performance (Figure 2L, unbalanced one-way $ANOVA_{TercMedSessILI}$ $F(2,573)=14.87$, $p<0.0005$; balanced one-way $ANOVA_{TercMedMiceILI}$ $F(2,153)=7.34$, $p=0.0009$; unbalanced one-way $ANOVA_{PerfMedSessILI}$ $F(2,573)=20.34$, $p<0.0005$; balanced one-way $ANOVA_{PerfMedMiceILI}$ $F(2,141)=9.92$, $p<0.0005$). These analyses indicate that mice do show improvements in waiting, but only during expert target-distractor discrimination performance. These comparisons of waiting and discrimination indicate potentially non-uniform learning trajectories for different task features, which we explore further below.

Transition in timing behavior. Next, we investigated the temporal strategy of reacting versus timing across learning. We test the hypothesis that, due to the post-stimulus lockout window, mice will transition from broad RT distributions to optimal timing behavior that aligns with the lockout duration. This addresses a temporal phenotype after a stimulus presentation. The null hypothesis predicts that mice learn to respond to a stimulus with the fastest RT distribution possible (reactive strategy, Figure 3A). Alternatively, we predict RT distributions to cluster at the lockout duration with decreased variance across learning (Figure 3B), indicating an improvement in timing.

We investigated reactive versus timing behavior by analyzing RT distributions across sessions and across tercile stages of training. We compared RT distributions for all stimulus responses (Figure 3C), for target premature responses (Figure 3D), and for target hit responses (Figure 3E). First, we describe response counts across training. Stimulus responses increased across training for all three distributions. For all stimulus responses, this was significant across all terciles (Figure 3C, unbalanced one-way $ANOVA_{TercStimResp}$ $F(2,573)=52.42$, $p<0.0005$; unbalanced one-way $ANOVA_{TercStimRT}$ $F(2,573)=51.11$, $p<0.0005$). Target premature responses increased significantly from early to middle terciles with a nonsignificant increase from middle to late terciles (Figure 3D, unbalanced one-way $ANOVA_{TercPremeTResp}$ $F(2,573)=9.90$, $p<0.0005$). Target hit responses increased across terciles as well (Figure 3E, unbalanced one-way $ANOVA_{TercHitsResp}$ $F(2,573)=105.66$, $p<0.0005$). Second, we note the timing of these distributions. All three response types increased their peak RT distribution at the 200 ms lockout restriction across terciles. To quantify this, we measured the mean reaction time across sessions and terciles (Figure 3F). As predicted by both the reactive and timing hypotheses, hits RTs significantly decreased across terciles (unbalanced one-way $ANOVA_{TercHitsRT}$ $F(2,569)=100.51$, $p<0.0005$). As uniquely predicted by the timing hypothesis, target premature RTs significantly increased from early to late terciles (unbalanced one-way $ANOVA_{TercPremeTRT}$ $F(2,545)=5.09$, $p=0.0065$). We also quantified timing per mouse by plotting outcome-based RT for each session across learning and determining the slopes of a linear fit (Figure 3F). We found that target premature RTs significantly increased while target hit RTs significantly decreased across sessions per mouse (one sample t-test $\mu_{mPremeTRT}=0.003\pm0.001$, $p=0.0008$; $\mu_{mHitsRT}=-0.023\pm0.002$, $p<0.0005$, $n=52$ mice). Although false alarm counts increased from early to middle tercile, all other distractor counts and RTs showed no difference across sessions or terciles (Supplementary Figure 1, unbalanced one-way $ANOVA_{TercFAResp}$ $F(2,573)=5.64$, $p=0.0038$). Additionally, distractor RTs did not change with training (Supplementary Figure 1C). These analyses demonstrate robust changes in post-stimulus behavior, with a bidirectional target RT change for precise timing as required by the lockout window.

As timing behavior improves, we would expect an RT distribution to shift towards the lockout duration with decreased variance (Figure 3G). We investigated the RT CDF and found it to shift left and decrease in variance across sessions, across mice, and across terciles towards the lockout period (Figure 3H-J). As described above, we also plotted CDF curves according to target-distractor stimulus discrimination. Interestingly, we found that RT CDF curves during naïve performance differed dramatically from CDF curves during intermediate and expert performance (Figure 3K). We quantified the shift in CDF curves by the median RT for both terciles and performance (Figure 3L, unbalanced one-way $ANOVA_{TercMedSessRT}$ $F(2,573)=48.44$, $p<0.0005$; balanced one-way $ANOVA_{TercMedMiceRT}$ $F(2,153)=22.77$, $p<0.0005$; unbalanced one-way $ANOVA_{PerfMedSessRT}$ $F(2,573)=159.34$, $p<0.0005$; balanced one-way $ANOVA_{PerfMedMiceRT}$ $F(2,141)=34.35$, $p<0.0005$). We quantified the variance in CDF curves by the spread from the median RT for both terciles and performance (unbalanced one-way $ANOVA_{TercSpreadSessRT}$ $F(2,573)=103.59$, $p<0.0005$; balanced one-way $ANOVA_{TercSpreadMiceRT}$ $F(2,153)=44.73$, $p<0.0005$; unbalanced one-way $ANOVA_{PerfSpreadSessRT}$ $F(2,573)=304.11$, $p<0.0005$; balanced one-way $ANOVA_{PerfSpreadMiceRT}$ $F(2,141)=68.69$, $p<0.0005$). These analyses indicate that mice do show improvements in timing. Unlike waiting behavior, improvements in timing appeared to lead expert target-distractor discrimination, providing further evidence for potential intermediate stages in learning.

Order of learning for individual transition trajectories. Mice improved through training in object-based measures as determined by the slopes of their linear fits across sessions (Supplementary Figure 2). Hit rates significantly increased across sessions and FA rates significantly decreased across sessions (one sample t-test $\mu_{mHitRate}=5.141\pm0.525$, $p<0.0005$; $\mu_{mFARate}=-0.686\pm0.266$, $p=0.0128$, $n=52$ mice). As expected, suboptimal

sampling decreased, as determined by reductions in spontaneous response rates (one sample t-test $\mu_{mSpontRate}$=-0.448±0.168, p=0.0101, n=52 mice). Additionally, we found that overall target detection significantly increased across sessions (one sample t-test $\mu_{md'Target}$=0.178±0.018, p<0.0005; $\mu_{mTPremed'}$=0.036±0.020, p=0.0737, n=52 mice). Also expected, target-distractor discrimination significantly increased and target-distractor criterion bias significantly decreased (one sample t-test $\mu_{md'Discrim}$=0.183±0.016, p<0.0005; μ_{mCBias}=-0.070±0.012, p<0.0005, n=52 mice).

While analyzing temporal and object-based measure through training, we noticed that different measures displayed distinct learning trajectories across mice (Figure 4A). Furthermore, some trajectories appeared to lag or lead others; for example, stimulus responding increased before waiting with discrimination increasing in between the two (Figure 4B). We investigated these learning dynamics using two methods. For both analyses we segregated training sessions into quintiles. In our first analysis, for individual measures per mouse, we determined the interquintile showing the maximum change. For example, early learning would be reflected in a maximum change between the first two quintiles, late learning between the last two quintiles (Figure 4B). Next, we binned the interquintile of maximum change for all mice (Figure 4C). We found that some distributions clustered towards the 1st interquintile (e.g., stimulus response rate), some towards the 4th interquintile (e.g., waiting), and others appeared evenly distributed across mice (e.g., distractor d', Figure 4C).

We compared the distributions of interquintiles of maximum change. This analysis yielded an ordered learning across our selected measures (Figure 4D). We interpret this as evidence for sequential transitions in strategy across learning. Maximum increases in stimulus response rates occurred significantly earlier than maximum increases in waiting ($\mu_{Resp\Delta max}$=1.98±0.13 versus $\mu_{Wait\Delta max}$=2.69±0.16, Kruskal-Wallis p=0.03, n=52 mice). Maximum increases were not significantly different between other paired trajectories. We acknowledge three contributing explanations for the partially overlapping sequence. First, a number of these transitions co-fluctuate and may reflect overlapping learning strategies (explored further below). Second, different learning strategies may occur in overlapping time windows. Notably, the overlapping trajectories include both temporal and object-based measures. Third, lack of separation between measures may be due to variation in learning transitions across mice. Cross-correlations for interquintiles of maximum change demonstrated a statistically significant correlation across mice (p=0.0003) but with high variability (μ_{CorrR}=0.03, n=52 mice). Overall, this analysis demonstrates a partially structured learning sequence across multiple outcome measures, well beyond the single measure (target-distractor discrimination) that initially motivated this task design.

The broad distribution in interquintiles of maximum change led us to question whether biological differences accounted for learning variability. We therefore performed the same analyses as above, but separately for sex and genotype. We observed significant differences in interquintile distributions for male versus female mice (Figure 5). The mean interquintiles of maximum change for males appeared to be substantially clustered in comparison with females; females show a progression of learning where stimulus responding leads and waiting lags (Figure 5A, rank sum Kruskal-Wallis$_{Male}$ p=0.949, rank sum Kruskal-Wallis$_{Female}$ p=0.0119). Notably, the interquintile of maximum change for waiting differed between males and females (Figure 5B, $\mu_{MaleWait\Delta max}$=2.39±0.20, $\mu_{FemaleWait\Delta max}$=3.24±0.26; rank sum Kruskal-Wallis$_{WaitMale|Female}$, p=0.0123). Main sex differences were found in stimulus responding, distractor detection, and prestimulus waiting (Figure 5C, unbalanced two-way ANOVA$_{Resp|Sex}$, p=0.034; ANOVA$_{d'Distract|Sex}$, p=0.0007; ANOVA$_{Wait|Sex}$, p=0.007). Additionally, we observed an interaction effect between sex and waiting (Figure 5C, bottom right, unbalanced two-way ANOVA$_{MaleWait|FemaleWait}$, p=0.024; longitudinal RANOVA$_{Sex|Wait}$, p=0.037), indicating different learning trajectories in males versus females for this measure. We recognize that the overlapping distributions of male mice could reflect either coincident learning or high variability across subjects resulting in broad distributions across the population. We find evidence for the latter. Female mice showed a small yet significant correlation in their interquintiles of maximum changes ($\mu_{CorrRFemale}$=0.104, p=0.0001, n=17 mice), indicating a shared learning structure. In contrast, male mice did not have correlated interquintiles of maximum change ($\mu_{CorrRMale}$=-0.027 p=0.53, n=31 mice), suggesting more variable (and idiosyncratic) learning profiles. Analyses of temporal and object-based measures identified significant genotype differences in timing, spontaneous response rates, and

waiting across learning quintiles, but we did not pursue this further (Supplementary Figure 3, $RANOVA_{Gene|Time}$, p=0.0049, $RANOVA_{Gene|Spont}$, p=0.045, $RANOVA_{Gene|Wait}$, p=0.0045).

Order of learning for pairwise transition trajectories. Our second method of quantifying learning dynamics involved pair-wise comparisons of temporal or object-based measures. First, we used pairwise correlation analyses to determine patterns of shared variance between measures within individual mice (Figure 6A). For further pairwise analyses, we selected measures with low shared variance: stimulus responding, discrimination, timing, distractor detection, and waiting. For these measures, we determined their relational order of learning by plotting their trajectories against each other. Based on the curvature of the pairwise comparisons, we could identify leading, lagging, or co-occurring learning transitions (Figure 6B). We defined an inner (within) quintile distance per mouse by calculating the mean of the 2nd, 3rd, and 4th quintile points to the linear fit between the 1st and 5th pairwise quintile segment. A significant deviation from zero of innerquintile distances would indicate a 'curvature' and thereby an order of learning between the pairwise measures.

By summing curvature columns across pairwise comparisons, we could approximate orders of learning across mice (Figure 6C). Consistent with the binned interquintile order of learning, the pairwise curvature analysis ordered stimulus responding before waiting (Figure 6D, $d_{Resp|Wait}$=-0.25 a.u., p=0.0001). Additionally, this analysis identified that stimulus responding leads discrimination and distractor detection, and that waiting lags timing (Bonferroni corrected: $d_{Resp|Discrim}$=-0.32 a.u., p<0.0005; $d_{Resp|d'Distract}$=-0.19 a.u., p=0.011; $d_{Time|Wait}$=-0.12 a.u., p=0.022). While we do observe some differences in the precise ordering of learning, both approaches indicate a learning structure where stimulus responding leads and waiting lags. Accordingly, potential intermediates consist of both temporal and object-based measures.

As with interquintile of maximum change distributions, the broad distribution of innerquintile curvature led us to analyze sex-specific differences in learning variability (Figure 7). Therefore, we conducted the curvature analyses separately for male and female mice, and again observed substantial differences in the ordering and clustering of the learned measures (Figure 7A). For the normalized quintile magnitudes, analyzing sex-specific longitudinal trajectories revealed that male mice transitioned their timing, distractor detection, and waiting behavior differently in comparison with female mice (Figure 7B, $RANOVA_{Sex|Time}$, p=0.042; $RANOVA_{Sex|d'Distract}$, p=0.038; $RANOVA_{Sex|Wait}$, p=0.0046). Like the interquintile findings, innerquintile curvature analyses showed that female mice, but not male mice, increased their stimulus response rates before they increased waiting (Figure 7C, Bonferroni corrected: $d_{FemaleResp|Wait}$=-0.13 a.u., p=0.010; $d_{MaleResp|Wait}$=-0.048 a.u., p=0.19; unbalanced two-way $ANOVA_{SexResp|Wait}$, p=0.025). Thus, both analytical measures demonstrate structure in ordered learning, with prominent sex differences in learning profiles.

Discussion

In this study we have shown changes in multiple temporal and object-based measures across learning as mice transition from naïve to expert performance during a whisker-based selective detection task. Regarding temporal measures, mice learn to both wait for a target stimulus and time after a target stimulus (Figure 2, Figure 3). Using individual trajectory (Figure 4) and pairwise trajectory (Figure 6) analyses, we identify structure in the changes of these measures that suggest an order or progression of learning. Interestingly, both approaches identify notable sex differences in learning, where females show more stereotypic progressions (Figures 5 and 7).

Based on our findings, we suggest that mice to not progress uniformly from naïve to expert across a single outcome measure (in our task, target-distractor discrimination). Instead, our data are more consistent with mice progressing through intermediate strategies. Based on our learning trajectory analyses, we propose a structure of learning that involves four distinct, yet temporally overlapping, behavior strategies or profiles as mice progress from naïve to expert performance (Figure 8). The first strategy of "naïve sampling" involves a general increase in responding, both before and after stimulus presentation. Evidence for this strategy includes an increase in all responding between early and middle terciles (Figure 2C,D,E) and the consistent finding across analyses of

increased stimulus responding leading all other measures (Figure 4C,D), followed closely by criterion bias. From a strategy of "naïve sampling", mice progress to "stimulus timing" (Figure 6C). The hallmark of this strategy is an improvement in RT, which ultimately centers around the onset of the response window (Figure 3D,E,F). The centering of RTs indicates that mice are responding to task-relevant stimuli, even if they continue high levels of random sampling. Mice then progress to "object-based performance", indicated by increases in specific responding to target stimuli (Figures 4D and 6C). Relevant measures of this strategy include increases in target detection and target-distractor discrimination (Figure 4A). Last is the strategy of "waiting and withholding". This stage of learning is evidenced by decreases in distractor detection and spontaneous responding and an improvement in waiting, which consistently lags in the progression (Figures 4C,D and 6C,D). In our task design, mice must wait between 5.5 to 14.6 seconds to receive a target stimulus and opportunity for reward. Therefore, waiting (not responding) through this ITI is critical for success in the task. And yet, increased waiting is typically the lagging transition in learning. This suggests that mice do not abandon a random sampling strategy until they are proficient in stimulus discrimination.

It is currently unclear whether these four strategies are truly discrete processes involving different neural mechanisms, and the extent to which these strategies generalize to different behavioral tasks. However, our findings strongly encourage taking a broader approach to the study of learning than is typically reported in behavioral neuroscience investigations. We identify three major reasons for promoting this approach. First, if there is an orderly progression of learning, then identifying the learning stages will aid in tracking the learning process. Second, and relatedly, mouse models of neuropsychiatric disease show learning deficits in goal-directed tasks (Goel et al., 2018; Hölter et al., 2015; Huynh et al., 2009; Remmelink et al., 2016). Are learning deficits due to failed progression across a specific stage of learning? Do different disease models fail at different learning stages, suggesting process-specific dysfunctions? Third, and perhaps most importantly, a growing number of studies are aimed at revealing the neuronal mechanisms underlying task learning (Huber et al., 2012; Lacefield et al., 2019; Le Merre et al., 2018; Makino et al., 2017; Roy et al., 2021). For example, increased activity in a brain region across learning in our task may be interpreted as a mechanism of target-distractor discrimination. However, considering this study, we recognize that changes in neuronal activity may also be related to general responding, timing, or impulse control (for both spontaneous and sensory-evoked responding). In future studies, correlating the trajectories of behavioral and neuronal measures may vastly improve our ability to identify the neuronal mechanisms underlying specific learning processes, and make more precise predictions about the effects of causal neuronal manipulations on learning outcomes.

Behavior modeling can confirm this potential, tracking task related performance processes across learning (Roy et al., 2021). Recent studies have provided great insights regarding strategies in expert performance with discrete state analyses (Ashwood et al., 2022; Pisupati et al., 2021). These types of analyses can be applied to the study of mixed (intermediate) states overlapping object-based and temporal strategies in learning. Even so, the investigation of learning strategies is often based on models presumed before interpretation. In this study, we do not predefine strategies in learning, only what can be inferred by behavior output measures. Our findings are empirical, identifying model-free mixed strategies, which may indicate intermediate neural mechanisms. With these approaches, considering raw behavioral measures enables impartial identification of diverse behavioral strategies across animal models and task paradigms.

Another insight from this study is the importance of considering temporal processes in object-based tasks. Our ITI distributions were meant to reduce temporal expectancy of target stimulus delivery (Coull et al., 2011; Fiorillo et al., 2008; Ghose & Maunsell, 2002; Nobre et al., 2007; Zariwala et al., 2013). Nevertheless, there remains temporal regularity in the structure of all behavioral tasks. Subjects may learn these temporal regularities to improve task performance by predicting windows of opportunity in task structure (Komiyama et al., 2010). However, subjects may also exploit these temporal regularities to solve a task in a way that was unintended (Kawai et al., 2015). By considering temporal processes in object-based tasks, researchers may reveal understudied task dimensions that are critical for optimal performance and strongly contribute to behavioral dysfunctions in neuropsychiatric disease (Emmons et al., 2017; Grondin, 2010; Toplak et al., 2006).

Across mice we recognize high variability in changes in performance measures, suggesting high variability in the progression through learning strategies. While expert mice converge to the same strategy (high discrimination, improved waiting, improved timing), individual mice do vary in their paths to expert performance. We are just beginning to explore the reasons for these individual differences. We note sex-based similarities and differences in learning trajectories. In both male and female mice, the strategy of naïve sampling tended to lead the other three strategies. For acquisition of the other three strategies, male mice were more idiosyncratic resulting in overlapping distributions of outcome measures, whereas females displayed more sequential stereotypy (Figure 5A, Figure 7A, Figure 8). Another interesting difference is a dissociation in two types of impulse control; female mice displayed lower distractor detection whereas male mice displayed higher ability to wait (Figure 5C). We do not know the cause of these sex differences, but they may relate to reported differences in novel environment exploration, in which females demonstrate more cautious (systematic) versus more risky (exploratory) decision-making behavior (Gagnon et al., 2016; Gagnon et al., 2018).

Materials and methods

Animals

Animal subjects

Experimental protocols have been approved by the IACUC of University of California, Riverside. The dataset used here include behavioral studies that have been previously reported (Aruljothi et al., 2020; Marrero et al., 2022; Zareian et al., 2022; Zareian et al., 2021; Zhang & Zagha, 2022). A wide variety of wild type and transgenic mice were considered for behavioral learning data. Male and female, wild type (C57BL/6J, JAX #000664; BALB/cByJ, JAX #001026), transgenic (Snap25-2A-GCaMP6s-D, JAX #025111; Thy1-ChR2-YFP, JAX #007612; VGAT-ChR2-EYFP, JAX #014548), and virus-injected adult mice were used (Arenkiel et al., 2007; Zhao et al., 2011). Mice were not under transgenic manipulation (e.g., optogenetic activation or Ca^{2+}-sensor imaging) during behavioral training. Mice were maintained in a 12-h light/dark cycle and animal behavior occurred during the light cycle. Mice were head-fixed before behavioral training began, as previously reported (Aruljothi et al., 2020; Zareian et al., 2021; Zhang & Zagha, 2022). Mice started behavioral training after a minimum of a 4-day recovery period from surgery.

Animal behavior

Training stages, metrics of learning, and criterion for expert performance in the Go/NoGo selective whisker detection task were as previously reported (Aruljothi et al., 2020). Briefly, head-fixed and water deprived mice learned on customized behavioral rigs. Behavioral data was collected using Arduino and custom MATLAB scripts (MathWorks, MA). Target and distractor paddles were positioned symmetrically within the mouse whisker fields bilaterally. Mice reported stimulus detection by licking a centrally located lick port, positioned under the snout. Mice progress through classical conditioning (2-5 days) and operant conditioning (2-5 days) stages before entering the full task (Figure 1, see Aruljothi et al., 2020 for details). Data presented in this paper are exclusively from the full task, in which the task structure did not change through training.

In the full task, we implemented a variable intertrial interval (ITI) before a stimulus presentation to discourage spontaneous sampling. Lick bouts within the ITI were punished by ending the trial and beginning the next trial with a new ITI, randomly selected from a negative exponential distribution between 5.5 and 9.5 s. Target stimuli and distractor stimuli were presented on a probabilistic schedule, 20% and 80% respectively. Following the correct rejection of a distractor stimulus, the next ITI was randomly selected from a negative exponential between 0.2 and 1.9 s. We also implemented a short lockout period (200-300 ms) after a stimulus presentation to isolate sensory versus response-related activity. Responding during the lockout ended the current trial and initiated a full ITI. Lick bouts, reaction times, stimulus types, and trial outcome types were recorded throughout the task. Lick bouts were considered spontaneous (sampling) if they occurred within the ITI. Post-stimulus licking responses were considered hits if they occurred after a target whisker stimulus and during the response window (after the lockout). Post-stimulus licking responses were considered false alarms (FA) or premature (Preme) if they occurred after a distractor whisker stimulus or during the lockout window, respectively. Hits (responses to

target stimuli) were rewarded with ~5 μL of water, correct rejections (not responding to distractor stimuli) and correct withholdings (not responding during the catch trial) were rewarded with a shortened intertrial-interval (ITI) and a subsequent target trial. Only trials of task engagement periods within sessions were analyzed, with 'task engagement' defined as a minimum block of 10 minutes without a pause in licking greater than 60 seconds. If more than one engagement period was identified within a session, the longest engagement period was chosen for the subsequent analyses. Spontaneous rates per session were calculated as the percentage of trial types in which the mouse responded within 1 second before an impending stimulus. Response rates per session were calculated as the percentage of response trial outcome types across all stimulus trials. Measures based on signal detection theory were calculated,

$$d'_{Stimulus\ Detection} = z_{Response\ Rate} - 1.2 * (z_{Spontaneous\ Rate})$$
$$d'_{Discrimination\ Performance} = z_{Hit\ Rate} - z_{False\ Alarm\ Rate}$$
$$d'_{Target\ Detection} = z_{Hit\ Rate} - z_{Spontaneous\ Rate}$$
$$d'_{Distractor\ Detection} = z_{False\ Alarm\ Rate} - z_{Spontaneous\ Rate}$$
$$d'_{Premature\ Detection} = z_{Premature\ Rate} - 0.2 * (z_{Spontaneous\ Rate})$$
$$C_{Criterion\ Bias} = -0.5 * (z_{Hit\ Rate} + z_{False\ Alarm\ Rate})$$

where z is the inverse normal distribution function.

Data inclusion criteria

We examined 120 mice with potential learning data but included only the 52 mice who met all criteria described below. First, mice were included if they learned the task, as defined by discrimination performance (d' between hit rate and false alarm rate) greater than one for three consecutive days. Second, mice were included if they learned progressively: from naïve to expert performance in less than three weeks of training. Third, the data required a minimum of seven training sessions with a maximum 7-day gap between sessions. No more than seven sessions of consecutive expert behavior were analyzed.

For tercile and quintile learning data per mouse, each session was binned according to the exclusive integer value of total sessions divided by three and five, respectively. For performance learning data per mouse, each session was defined as naïve (d'<0.8), intermediate (0.8<d'<1.2), and expert (d'>1.2). The intermediate performance was considered because it highlighted performance near our learning threshold. This allowed for comparison of time in training (tercile or quintile) versus learning stage (performance), with the potential of identifying intermediate behavioral strategies. Sex-specificity in learning was studied according to available data on the sex of each mouse (available for 48 of the 52 total mice).

Behavioral learning analyses

Analyses were performed using standard MATLAB scripts. Linear regression analyses were used to determine slopes of behavioral outcome measures across sessions per mouse (Figures 2, 3, and Supplementary 1, 2). If linear slopes across mice were significantly positive, the transition was identified as 'increasing'; if linear slopes across mice were significantly negative, the transition was identified as 'decreasing'.

For individual trajectory analyses (Figures 4 and 5), interquintiles of maximum change were determined as the differential slopes across quintiles ($\Delta_{Trajectory}/\Delta_{quintile}$) per mouse. Interquintiles were then binned categorically for interquintile analysis. Order of learning was specified by ordering the mean interquintiles across mice per measure.

Behavioral measures with non-redundant dynamics (Figure 6) were identified by correlation analyses (MATLAB function *corrcoef*) for measures across quintiles per mouse, and then averaged across mice. We considered the absolute value of the correlations to determine magnitude of correlation (or anticorrelation). High correlations indicated measures with similar dynamics; low correlations indicated measures with unique dynamics and were therefore included in pairwise trajectory analyses.

For pairwise trajectory analyses (Figures 6 and 7), innerquintile curvature was determined by first rectifying quintile points such that quintiles increased by the absolute value of consecutive interquintile changes,

+abs($\Delta_{Trajectory}$); rectified quintile points were then scaled to the interval [0 1]. Then, pairwise transition quintiles were plotted against each other. Innerquintile curvature was defined as the mean distance of pairwise quintile points 2, 3, and 4 to the line segment between pairwise quintile points 1 and 5 per mouse.

Strategies in Figure 8 were identified as combinations of individual measures, based on assessments of both individual and pairwise trajectory analyses.

Statistical analyses

Reproducibility of learning data

Session performance was reported for all learning sessions per mouse, jittered only for visualization and not for quantification. For interlick interval (ILI) analysis, the term 'sampling' was defined by the percent area under the histogram curve of spontaneous lick bouts between zero and the minimum ITI per session. For most sessions, this was between zero and 5.5 seconds. The term 'waiting' was defined by the percent area under the histogram curve of stimulus responses between the minimum ITI per session and the maximum possible wait time for engaged behavior per session. For most sessions, this was between 5.5 and 14.6 seconds (9.5 s maximum ITI for distractor stimulus, 2.2 s for subsequent correct rejection trial, 1.9 s for maximum shortened ITI, 1 s for prestimulus trial window preceding a target stimulus). For rection time analyses, reaction times in premature trials were defined by the lockout period per session. For most mice, this was 0.2 seconds (0.3 seconds for 3 mice). Stimulus response trials were determined by reaction times greater than the lockout period and during the 1 second response window. Data are reported as mean ± standard error of the mean (SEM) unless otherwise noted. Cumulative probabilities per session, per tercile, per tercile per mouse, and by performance level were determined by cumulative distribution functions (CDFs), the normalized cumulative sum under ILI or RT distributions. Because interlick and reaction time distributions were not gaussian, the median values (instead of means) are reported. To report spread in reaction time distributions, the spread of ±34.1% from the median was used to emulate one standard deviation in the nongaussian distribution.

Statistics for learning data

All analyses, including statistics, were performed using standard and custom MATLAB scripts and visualized using CorelDRAW. One sample t-tests were used to determine if slopes across mice were significantly different from zero (MATLAB function *ttest*). Nonparametric (interquintile of maximum change in trajectory) data were analyzed using the chi-square (χ^2) Kruskal-Wallis rank sum test (MATLAB function *kruskalwallis*) across all measures for all mice, male mice, and female mice. For the waiting measure specified by sex, Kruskal-Wallis rank sum was performed on the nonparametric waiting data for all males versus all females. Cross correlation analyses were performed for interquintiles of maximum change across all mice, across male mice, and across female mice, separately, by determining the correlation coefficient (MATLAB function *corrcoef*). Reported correlations are calculated from the mean correlation. One sample t-test was used for analyses of innerquintile curvature across all mice to test significant curvature difference from zero, Bonferroni corrected for multiple comparisons. For analysis of variance (ANOVA) statistical tests (balanced and unbalanced one-way ANOVA, two-way ANOVA, and longitudinal RANOVA), Tukey-Kramer post-hoc multiple comparisons were generated using function *multcompare* in MATLAB. Significance was assigned according to p-values <0.05. For visualization, asterisks are shown according to orders of p-values: *p<0.05, **p<0.005, ***p<0.0005.

Acknowledgements

This work was supported by the Whitehall Foundation (Research Grant 2017-05-71 to E.Z.) and the National Institutes of Health (R01NS107599 to E.Z.). We thank Drs. Hongdian Yang and Anubhuti Goel for many helpful discussions throughout the project.

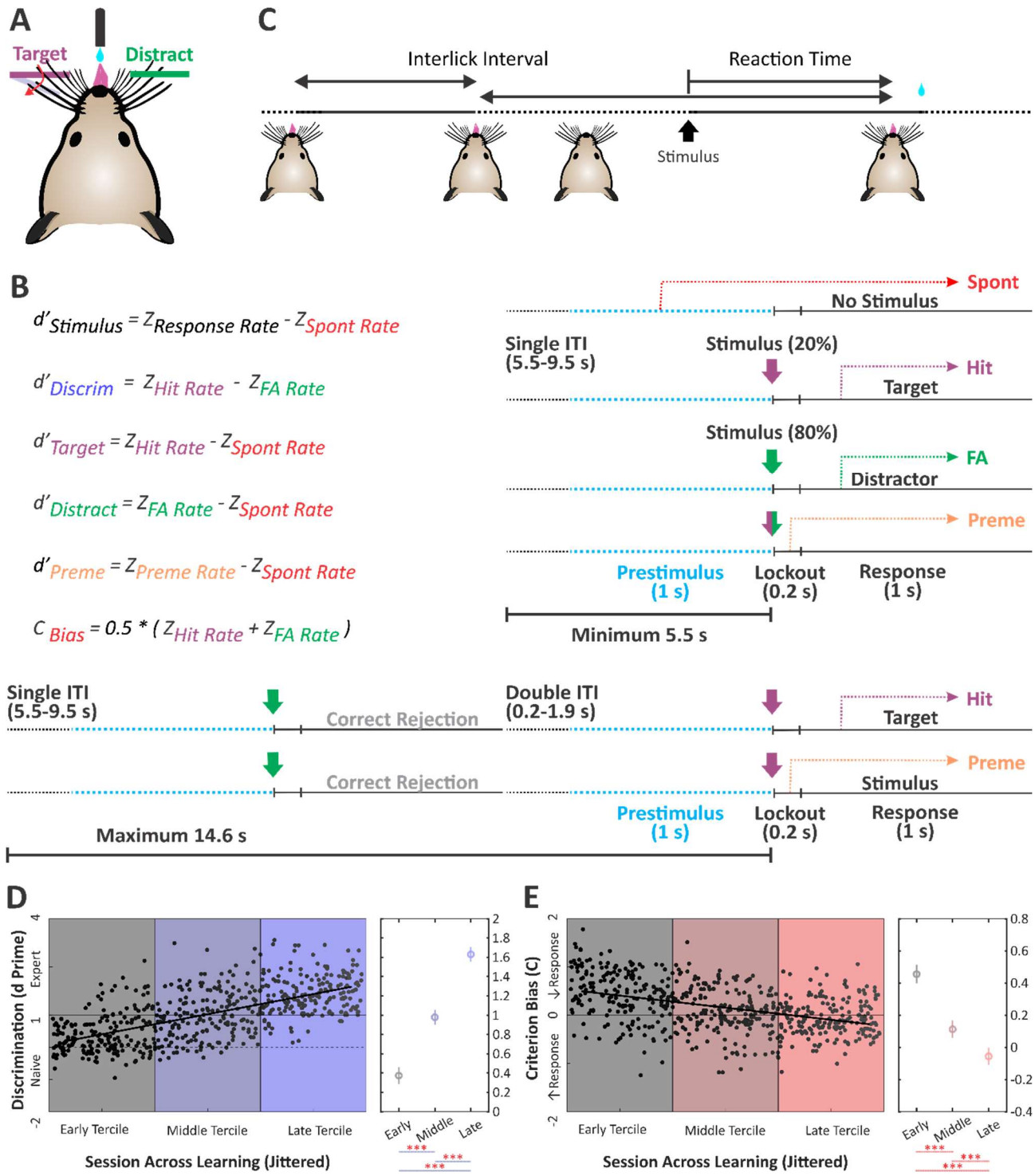

Figure 1: Trial structure, performance measures, and training data. *A) Mice learn to selectively respond to target whisker deflections (fuchsia) and ignore distractor whisker deflections (green). B) Signal detection measures were quantified according to response rates: Spontaneous (Spont, red) response during the ITI and before stimulus presentation; Hit (fuchsia) response after a target stimulus during the response window; False alarm (FA, green) response after a distractor stimulus during the response window; Premature (Preme, orange) response after a stimulus during the lockout period. C) Strategies were investigated according to interlick intervals (temporal distance between consecutive licks) and reaction times (temporal distance between stimulus presentation and response). D) (Left) discrimination performance plotted across all sessions and all mice, segregated according to duration in training (early, middle, late); (right) quantification of tercile means across sessions. E) Same dataset and layout as in D, but for criterion bias. Shading denotes progression in training by tercile, dark to bright. (Unbalanced one-way ANOVA with post-hoc multiple comparisons *** p<0.0005).*

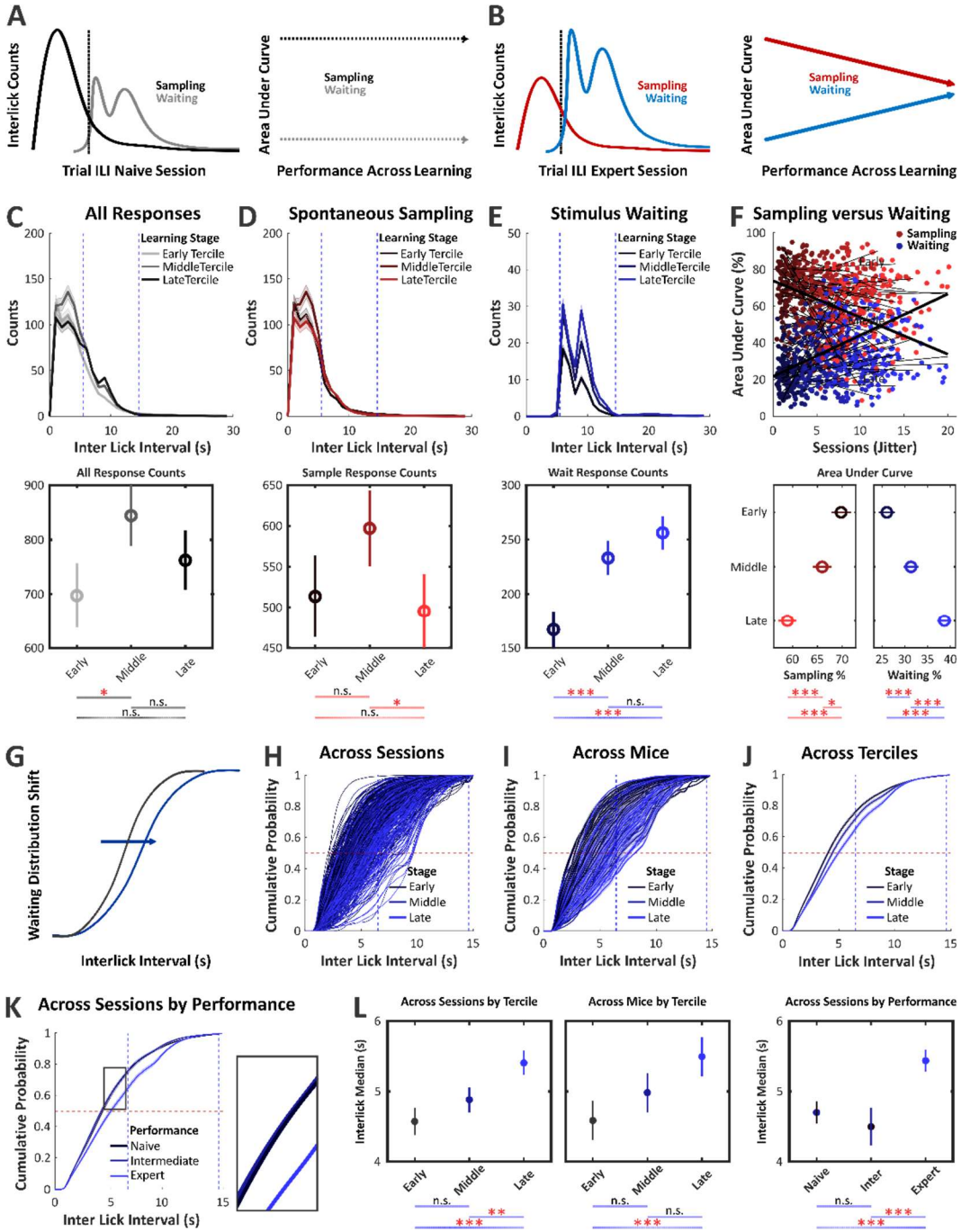

Figure 2: Mice transition from a sampling to waiting strategy before stimulus presentation across learning. *A) (Left) hypothetical example of response distributions in naïve behavior before learning; (right) longitudinal performance if response behavior does not change across learning. B) (Left) hypothetical example of response distribution in expert behavior after learning; (right) longitudinal performance if response behavior changes across learning. C) Mice increase and then decrease all responding across terciles; shading denotes progression in training (grey to black). D) Mice decrease spontaneous prestimulus sampling from middle to late terciles. E) Mice increase stimulus responding from early to middle terciles. F) Percent area under the curve (%AUC) per session of spontaneous sampling (red) and stimulus waiting (blue) with linear fits across sessions per mouse (faint black) and mean of linear fits across mice (bold black). G) Expected cumulative distribution function shift if waiting behavior changes across learning. H) Cumulative probability distribution function (CDF) curves across all sessions. I) CDF curves across terciles per mouse. J) Mean CDF curves across tercile sessions. K) Mean CDF curves across performance sessions; inset shows overlapping of naïve and intermediate performance CDFs. L) Quantification of tercile means across sessions, tercile means across mice, and performance means across all sessions. [D-K] Shading denotes progression in training by session, dark to bright. (Balanced and unbalanced one-way ANOVA with post-hoc multiple comparisons * $p<0.05$, ** $p<0.005$, *** $p<0.0005$, n.s. $p>0.05$).*

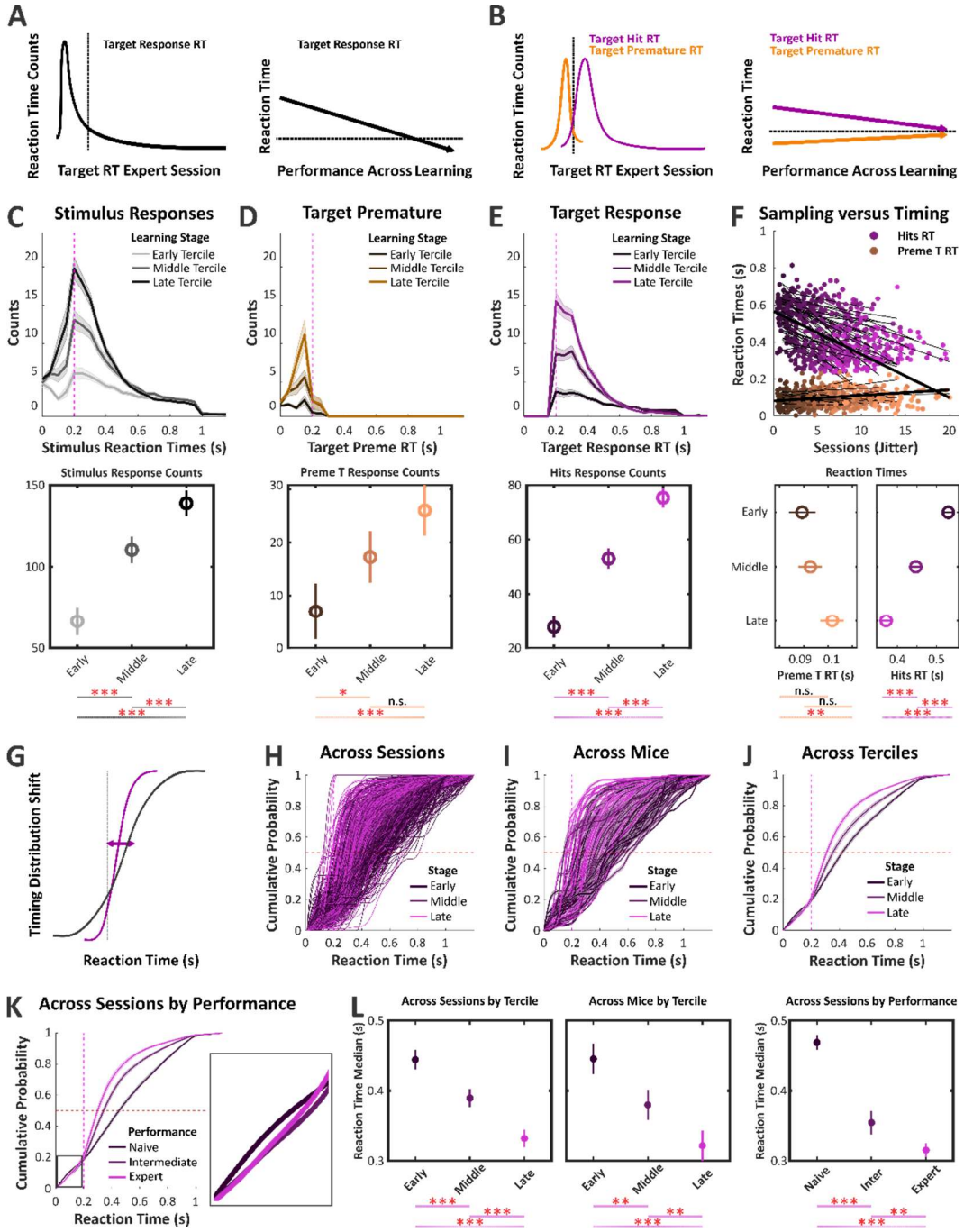

Figure 3: Mice transition from a sampling to timing strategy after stimulus presentation across learning. *A) (Left) hypothetical example of RT distribution in mouse behavior before and after learning if target RT improves to fastest RT possible; (right) longitudinal performance if RTs decrease across learning. B) (Left) hypothetical example of RT distribution in mouse behavior after learning if RTs converge to the imposed lockout period (dashed gray line); (right) longitudinal performance if RTs converge to the lockout period across learning. C) Mice increase stimulus responses across terciles; shading denotes progression in training, grey to black. D) Mice increase target premature (orange) RT counts across terciles. E) Mice increase target hits RT counts across terciles. For all RT distributions (C-E), the maximum increase is at the time of the lockout (vertical line). F) Target stimulus RTs per session for hits and target premature trials with linear fits across sessions per mouse (faint black) and mean of linear fits across mice (bold black). G) Expected cumulative distribution function shift if timing behavior changes across learning. H) Cumulative probability distribution function (CDF) curves across all sessions. I) CDF curves across terciles per mouse. J) Mean CDF curves across tercile sessions. K) Mean CDF curves across performance sessions; inset shows overlapping of naïve and intermediate performance CDFs. L) Quantification of tercile means across sessions, tercile means across mice, and performance means across sessions. [D-K] Shading denotes progression in training, dark to bright. (Balanced and unbalanced ne-way ANOVA with post-hoc multiple comparisons * $p<0.05$, ** $p<0.005$, *** $p<0.0005$, n.s. $p>0.05$).*

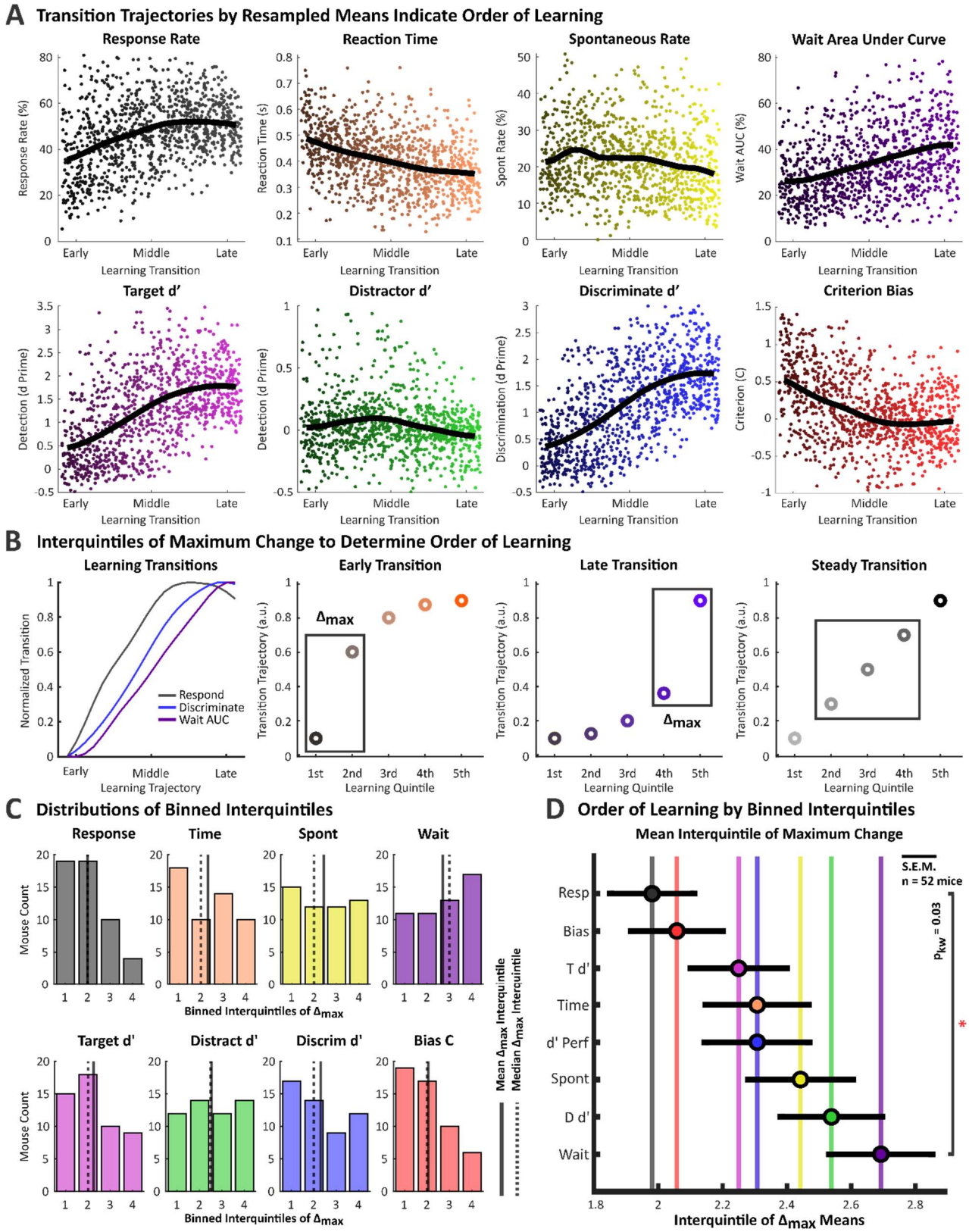

Figure 4: Interquintile of maximum change analyses reveal order of learning. *A) Resampled means of object-based and temporal transition trajectories across mice: stimulus response rate (grey); RT (orange); spontaneous rate (yellow); wait AUC (purple); target detection (fuchsia); distractor detection (green); discrimination (blue); criterion (red); shading denotes progression in learning by resampled sessions, dark to bright. B) Normalized increasing trajectories for stimulus responding, discriminating, and waiting; example interquintile transitions: early, late, steady transitions. C) Distributions of interquintile of maximum change per measure across mice. D) Mean interquintile of maximum change ($\mu_{\Delta max} \pm$ S.E.M.) sequenced by increasing order (Kruskal Wallis rank sum ANOVA * $p<0.05$).*

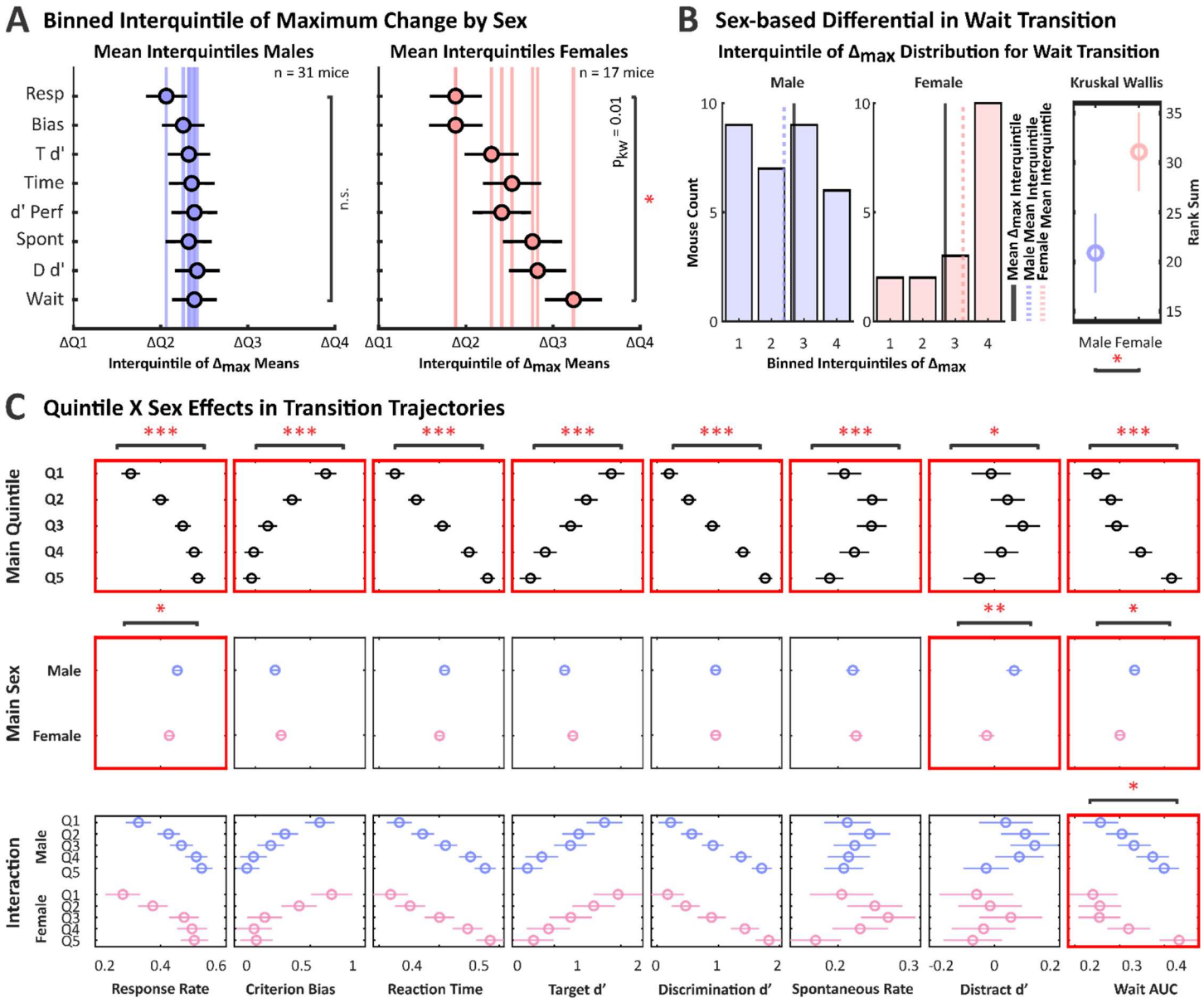

Figure 5: Order of learning by interquintile of maximum change exhibits sex specificity. *A) Male versus female mean interquintile of maximum change ($\mu_{\Delta max}$ ± S.E.M.) sequenced as in* ***Figure 4****. B) Male versus female distributions of interquintile of maximum change for wait AUC; solid line, all mice mean interquintile; dashed line, male/female mean interquintile. C) Transitions of each measure by quintile (top), sex (middle), and quintile X sex interactions (bottom); colors: blue – male, pink – female. (Kruskal Wallis rank sum by sex * p<0.05; unbalanced two-way ANOVA with post-hoc multiple comparisons * p<0.05, ** p<0.005, *** p<0.0005; red borders indicate significance).*

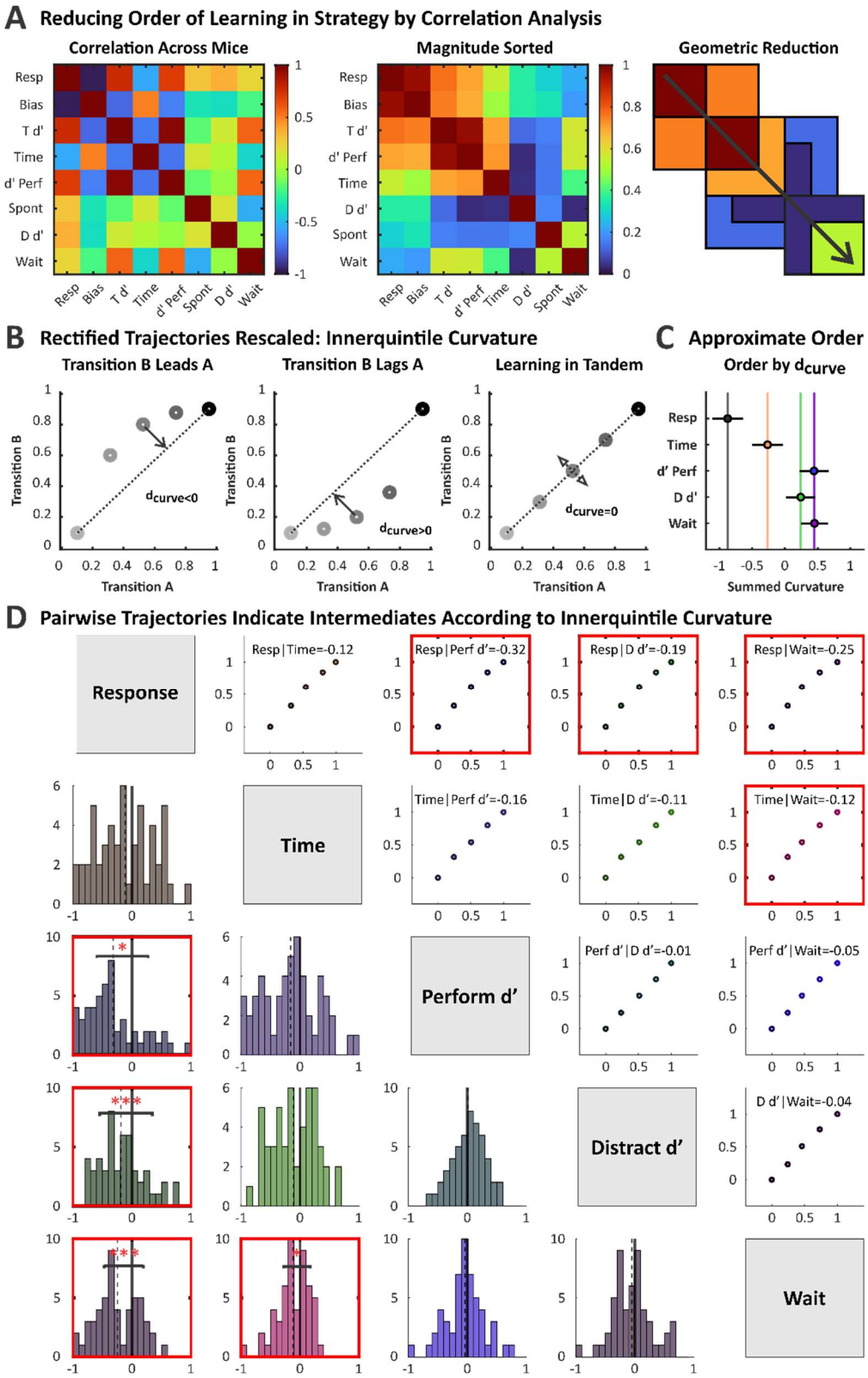

Figure 6: Pairwise innerquintile curvature reveals intermediates in the order of learning. *A) Correlations of measures across mice, color scale [-1 1] (left); sorted correlation magnitudes across mice, color scale [0 1] (middle); geometric reduction model of sorted correlation magnitudes (right). B) Example analyses for innerquintile curvature (d_{curve}) between rectified pairwise measures by quintile (see Methods and Materials). C) Summed d_{curve} across columns in (D); $\sum \mu_{dcurve} \pm$ S.E.M. for learning order approximation. D) Pairwise innerquintile curvature and distributions across mice (top-right, mean d_{curve} across pairwise comparisons; bottom-left, d_{curve} distributions; dashed line, mean d_{curve} across distribution. (One sample t-test, Bonferroni corrected: * $p<0.05$, *** $p<0.0005$; red borders indicate significant curvature, denoting differences in learning trajectories).*

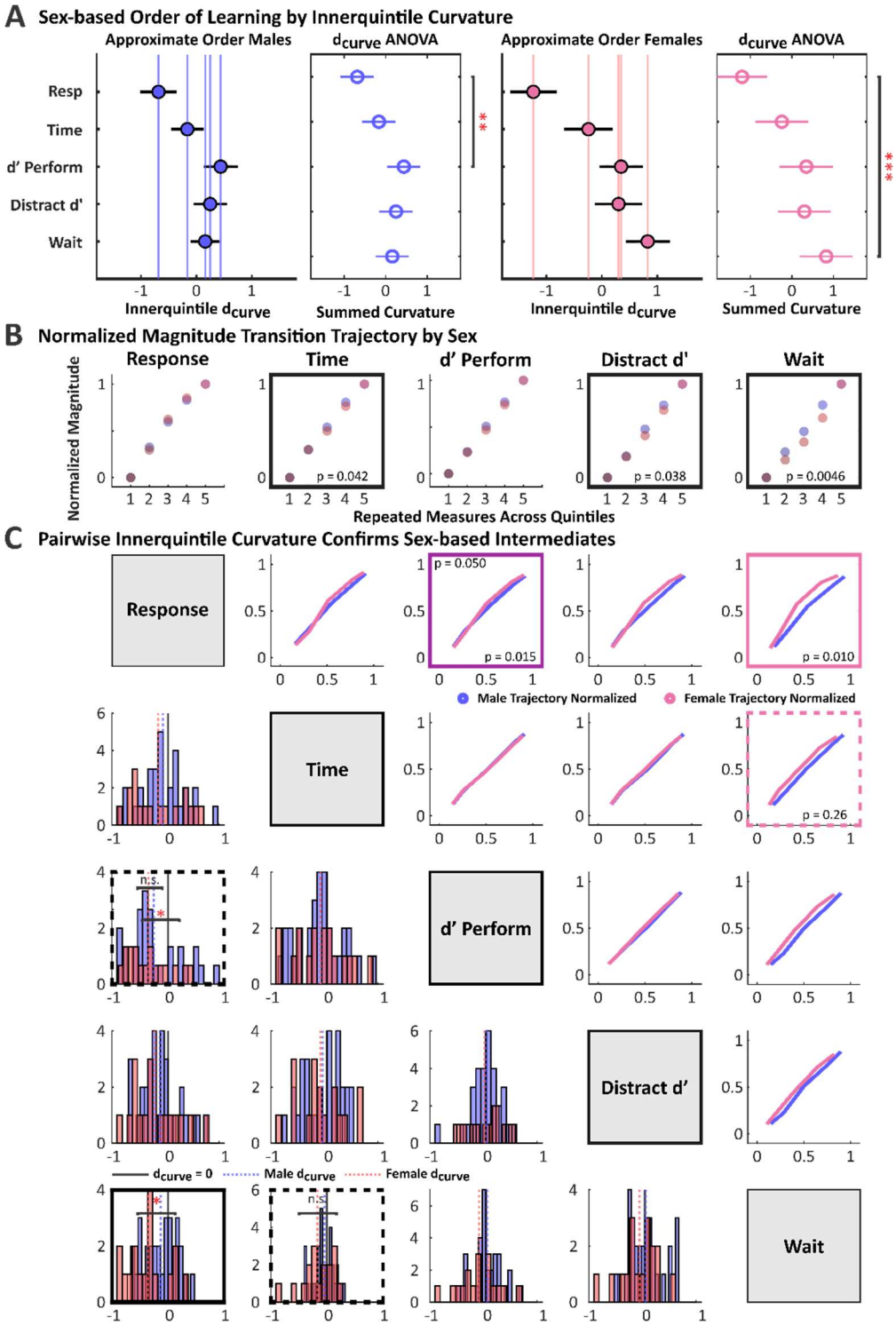

Figure 7: Order of learning by pairwise innerquintile curvature exhibits sex specificity. A) *Male versus female: summed d_{curve} across columns in (C); $\sum\mu_{dcurve} \pm$ S.E.M. for learning order approximation. B) Male versus female normalized learning trajectories across quintiles for individual measures; black borders denote statically significant differences (repeated measures ANOVA for longitudinal trajectories). C) Pairwise innerquintile curvature and distributions by sex (top-right, mean d_{curve} across pairwise comparisons by sex; bottom-left, d_{curve} distributions by sex; colored dashed lines, mean d_{curve} across distribution by sex; black dashed line, $d_{curve} = 0$; colors: blue – male, pink – female. (One sample t-test ** $p<0.005$, *** $p<0.0005$, border in pink denotes significant curvature in female but not male mice, border in purple denotes significant curvature in both male and female mice; unbalanced one-way ANOVA * $p<0.05$, n.s. $p<0.10$, border in black denotes significant difference between male versus female d_{curve}, dashed border denotes nonsignificant but noteworthy comparisons between male versus female d_{curve}).*

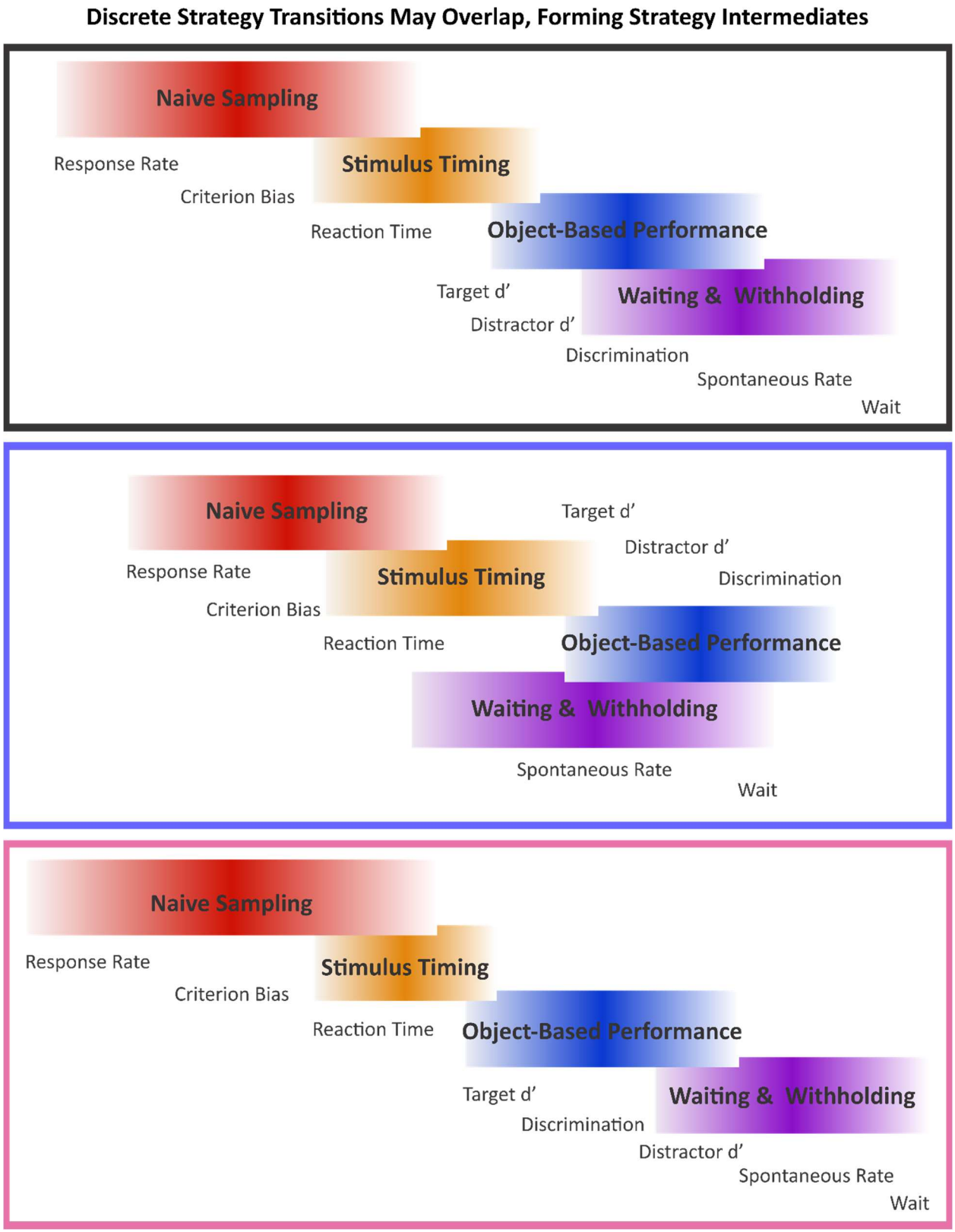

Figure 8: Object-based and temporal transitions overlap, forming intermediate behavioral strategies. *A) General learning strategy framework in which an initial strategy of naïve sampling progresses to stimulus timing, object-based performance, and ultimately waiting and withholding. B) Learning strategy framework for male mice in which naïve sampling overlaps with stimulus timing and waiting and withhold intermediates, following by object-based performance. C) Learning strategy framework for female mice in which the intermediate strategies are more temporally distinct.*

Arenkiel, B. R., Peca, J., Davison, I. G., Feliciano, C., Deisseroth, K., Augustine, George J. J., Ehlers, M. D., & Feng, G. (2007). In Vivo Light-Induced Activation of Neural Circuitry in Transgenic Mice Expressing Channelrhodopsin-2. *Neuron*, *54*(2), 205-218. https://doi.org/10.1016/j.neuron.2007.03.005

Aruljothi, K., Marrero, K., Zhang, Z., Zareian, B., & Zagha, E. (2020). Functional Localization of an Attenuating Filter within Cortex for a Selective Detection Task in Mice. *The Journal of Neuroscience*, *40*(28), 5443-5454. https://doi.org/10.1523/jneurosci.2993-19.2020

Ashwood, Z. C., Roy, N. A., Stone, I. R., International Brain, L., Urai, A. E., Churchland, A. K., Pouget, A., & Pillow, J. W. (2022). Mice alternate between discrete strategies during perceptual decision-making. *Nat Neurosci*, *25*(2), 201-212. https://doi.org/10.1038/s41593-021-01007-z

Bakhurin, K. I., Goudar, V., Shobe, J. L., Claar, L. D., Buonomano, D. V., & Masmanidis, S. C. (2017). Differential Encoding of Time by Prefrontal and Striatal Network Dynamics. *J Neurosci*, *37*(4), 854-870. https://doi.org/10.1523/JNEUROSCI.1789-16.2016

Bari, A., & Robbins, T. W. (2013). Inhibition and impulsivity: behavioral and neural basis of response control. *Prog Neurobiol*, *108*, 44-79. https://doi.org/10.1016/j.pneurobio.2013.06.005

Baunez, C., & Robbins, T. W. (1997). Bilateral Lesions of the Subthalamic Nucleus Induce Multiple Deficits in an Attentional Task in Rats [https://doi.org/10.1111/j.1460-9568.1997.tb01376.x]. *European Journal of Neuroscience*, *9*(10), 2086-2099. https://doi.org/https://doi.org/10.1111/j.1460-9568.1997.tb01376.x

Baunez, C., & Robbins, T. W. (1999). Effects of transient inactivation of the subthalamic nucleus by local muscimol and APV infusions on performance on the five-choice serial reaction time task in rats. *Psychopharmacology*, *141*(1), 57-65. https://doi.org/10.1007/s002130050806

Bayard, F., Nymberg Thunell, C., Abe, C., Almeida, R., Banaschewski, T., Barker, G., Bokde, A. L. W., Bromberg, U., Buchel, C., Quinlan, E. B., Desrivieres, S., Flor, H., Frouin, V., Garavan, H., Gowland, P., Heinz, A., Ittermann, B., Martinot, J. L., Martinot, M. P., . . . Consortium, I. (2020). Distinct brain structure and behavior related to ADHD and conduct disorder traits. *Mol Psychiatry*, *25*(11), 3020-3033. https://doi.org/10.1038/s41380-018-0202-6

Buhusi, C. V., & Meck, W. H. (2005). What makes us tick? Functional and neural mechanisms of interval timing. *Nat Rev Neurosci*, *6*(10), 755-765. https://doi.org/10.1038/nrn1764

Carroll, C. A., O'Donnell, B. F., Shekhar, A., & Hetrick, W. P. (2009). Timing dysfunctions in schizophrenia as measured by a repetitive finger tapping task. *Brain Cogn*, *71*(3), 345-353. https://doi.org/10.1016/j.bandc.2009.06.009

Chen, T. W., Li, N., Daie, K., & Svoboda, K. (2017). A Map of Anticipatory Activity in Mouse Motor Cortex. *Neuron*, *94*(4), 866-879 e864. https://doi.org/10.1016/j.neuron.2017.05.005

Churchland, A. K., Kiani, R., Chaudhuri, R., Wang, X. J., Pouget, A., & Shadlen, M. N. (2011). Variance as a signature of neural computations during decision making. *Neuron*, *69*(4), 818-831. https://doi.org/10.1016/j.neuron.2010.12.037

Coull, J. T., Cheng, R. K., & Meck, W. H. (2011). Neuroanatomical and neurochemical substrates of timing. *Neuropsychopharmacology*, *36*(1), 3-25. https://doi.org/10.1038/npp.2010.113

Cravo, A. M., Rohenkohl, G., Santos, K. M., & Nobre, A. C. (2017). Temporal Anticipation Based on Memory. *J Cogn Neurosci*, *29*(12), 2081-2089. https://doi.org/10.1162/jocn_a_01172

Daw, N. D., Niv, Y., & Dayan, P. (2005). Uncertainty-based competition between prefrontal and dorsolateral striatal systems for behavioral control. *Nat Neurosci*, *8*(12), 1704-1711. https://doi.org/10.1038/nn1560

Dent, M. F., & Neill, D. B. (2012). Dose-dependent effects of prefrontal dopamine on behavioral state in rats. *Behav Neurosci*, *126*(5), 620-639. https://doi.org/10.1037/a0029640

Dickinson, A., & Balleine, B. W. (1994). Motivational control of goal-directed action. *Animal Learning & Behavior*, *22*, 1-18.

Droit-Volet, S., Meck, W. H., & Penney, T. B. (2007). Sensory modality and time perception in children and adults. *Behav Processes*, *74*(2), 244-250. https://doi.org/10.1016/j.beproc.2006.09.012

Duan, C. A., Erlich, J. C., & Brody, C. D. (2015). Requirement of Prefrontal and Midbrain Regions for Rapid Executive Control of Behavior in the Rat. *Neuron*, *86*(6), 1491-1503. https://doi.org/10.1016/j.neuron.2015.05.042

Eden, G. F., Stein, J. F., Wood, H. M., & Wood, F. B. (1995). Temporal and Spatial Processing in Reading Disabled and Normal Children. *Cortex*, *31*(3), 451-468. https://doi.org/https://doi.org/10.1016/S0010-9452(13)80059-7

Emmons, E. B., De Corte, B. J., Kim, Y., Parker, K. L., Matell, M. S., & Narayanan, N. S. (2017). Rodent Medial Frontal Control of Temporal Processing in the Dorsomedial Striatum. *J Neurosci*, *37*(36), 8718-8733. https://doi.org/10.1523/JNEUROSCI.1376-17.2017

Erlich, J. C., Bialek, M., & Brody, C. D. (2011). A cortical substrate for memory-guided orienting in the rat. *Neuron*, *72*(2), 330-343. https://doi.org/10.1016/j.neuron.2011.07.010

Erlich, J. C., Brunton, B. W., Duan, C. A., Hanks, T. D., & Brody, C. D. (2015). Distinct effects of prefrontal and parietal cortex inactivations on an accumulation of evidence task in the rat. *Elife*, *4*. https://doi.org/10.7554/eLife.05457

Fiorillo, C. D., Newsome, W. T., & Schultz, W. (2008). The temporal precision of reward prediction in dopamine neurons. *Nat Neurosci*, *11*(8), 966-973. https://doi.org/10.1038/nn.2159

Fiorillo, C. D., Tobler, P. N., & Schultz, W. (2003). Discrete Coding of Reward Probability and Uncertainty by Dopamine Neurons. *Science*, *299*(5614), 1898-1902. https://doi.org/doi:10.1126/science.1077349

Freedman, D. J., Riesenhuber, M., Poggio, T., & Miller, E. K. (2003). A Comparison of Primate Prefrontal and Inferior Temporal Cortices during Visual Categorization. *The Journal of Neuroscience*, *23*(12), 5235-5246. https://doi.org/10.1523/jneurosci.23-12-05235.2003

Gagnon, K. T., Cashdan, E. A., Stefanucci, J. K., & Creem-Regehr, S. H. (2016). Sex Differences in Exploration Behavior and the Relationship to Harm Avoidance. *Hum Nat*, *27*(1), 82-97. https://doi.org/10.1007/s12110-015-9248-1

Gagnon, K. T., Thomas, B. J., Munion, A., Creem-Regehr, S. H., Cashdan, E. A., & Stefanucci, J. K. (2018). Not all those who wander are lost: Spatial exploration patterns and their relationship to gender and spatial memory. *Cognition*, *180*, 108-117. https://doi.org/10.1016/j.cognition.2018.06.020

Ghose, G. M., & Maunsell, J. H. R. (2002). Attentional modulation in visual cortex depends on task timing. *Nature*, *419*(6907), 616-620. https://doi.org/10.1038/nature01057

Goel, A., Cantu, D. A., Guilfoyle, J., Chaudhari, G. R., Newadkar, A., Todisco, B., de Alba, D., Kourdougli, N., Schmitt, L. M., Pedapati, E., Erickson, C. A., & Portera-Cailliau, C. (2018). Impaired perceptual learning in a mouse model of Fragile X syndrome is mediated by parvalbumin neuron dysfunction and is reversible. *Nature Neuroscience*, *21*(10), 1404-1411. https://doi.org/10.1038/s41593-018-0231-0

Grabenhorst, M., Michalareas, G., Maloney, L. T., & Poeppel, D. (2019). The anticipation of events in time. *Nature Communications*, *10*(1), 5802. https://doi.org/10.1038/s41467-019-13849-0

Grondin, S. (2010). Timing and time perception: a review of recent behavioral and neuroscience findings and theoretical directions. *Atten Percept Psychophys*, *72*(3), 561-582. https://doi.org/10.3758/APP.72.3.561

Guo, Z. V., Li, N., Huber, D., Ophir, E., Gutnisky, D., Ting, J. T., Feng, G., & Svoboda, K. (2014). Flow of cortical activity underlying a tactile decision in mice. *Neuron*, *81*(1), 179-194. https://doi.org/10.1016/j.neuron.2013.10.020

Hanisch, C., Radach, R., Holtkamp, K., Herpertz-Dahlmann, B., & Konrad, K. (2006). Oculomotor inhibition in children with and without attention-deficit hyperactivity disorder (ADHD). *J Neural Transm (Vienna)*, *113*(5), 671-684. https://doi.org/10.1007/s00702-005-0344-y

Hölter, S. M., Garrett, L., Einicke, J., Sperling, B., Dirscherl, P., Zimprich, A., Fuchs, H., Gailus-Durner, V., Hrabě de Angelis, M., & Wurst, W. (2015). Assessing Cognition in Mice [https://doi.org/10.1002/9780470942390.mo150068]. *Current Protocols in Mouse Biology*, *5*(4), 331-358. https://doi.org/https://doi.org/10.1002/9780470942390.mo150068

Huber, D., Gutnisky, D. A., Peron, S., O'Connor, D. H., Wiegert, J. S., Tian, L., Oertner, T. G., Looger, L. L., & Svoboda, K. (2012). Multiple dynamic representations in the motor cortex during sensorimotor learning. *Nature*, *484*(7395), 473-478. https://doi.org/10.1038/nature11039

Huynh, D. P., Maalouf, M., Silva, A. J., Schweizer, F. E., & Pulst, S. M. (2009). Dissociated Fear and Spatial Learning in Mice with Deficiency of Ataxin-2. *PLoS One*, *4*(7), e6235. https://doi.org/10.1371/journal.pone.0006235

Jin, X., & Costa, R. M. (2010). Start/stop signals emerge in nigrostriatal circuits during sequence learning. *Nature*, *466*(7305), 457-462. https://doi.org/10.1038/nature09263

Kable, J. W., & Glimcher, P. W. (2007). The neural correlates of subjective value during intertemporal choice. *Nat Neurosci*, *10*(12), 1625-1633. https://doi.org/10.1038/nn2007

Kawai, R., Markman, T., Poddar, R., Ko, R., Fantana, A. L., Dhawale, A. K., Kampff, A. R., & Olveczky, B. P. (2015). Motor cortex is required for learning but not for executing a motor skill. *Neuron*, *86*(3), 800-812. https://doi.org/10.1016/j.neuron.2015.03.024

Komiyama, T., Sato, T. R., O'Connor, D. H., Zhang, Y. X., Huber, D., Hooks, B. M., Gabitto, M., & Svoboda, K. (2010). Learning-related fine-scale specificity imaged in motor cortex circuits of behaving mice. *Nature*, *464*(7292), 1182-1186. https://doi.org/10.1038/nature08897

Lacefield, C. O., Pnevmatikakis, E. A., Paninski, L., & Bruno, R. M. (2019). Reinforcement Learning Recruits Somata and Apical Dendrites across Layers of Primary Sensory Cortex. *Cell Rep*, *26*(8), 2000-2008 e2002. https://doi.org/10.1016/j.celrep.2019.01.093

Lak, A., Costa, G. M., Romberg, E., Koulakov, A. A., Mainen, Z. F., & Kepecs, A. (2014). Orbitofrontal cortex is required for optimal waiting based on decision confidence. *Neuron*, *84*(1), 190-201. https://doi.org/10.1016/j.neuron.2014.08.039

Laubach, M., Wessberg, J., & Nicolelis, M. A. L. (2000). Cortical ensemble activity increasingly predicts behaviour outcomes during learning of a motor task. *Nature*, *405*(6786), 567-571. https://doi.org/10.1038/35014604

Lawson, R. P., Bisby, J., Nord, C. L., Burgess, N., & Rees, G. (2021). The Computational, Pharmacological, and Physiological Determinants of Sensory Learning under Uncertainty. *Curr Biol*, *31*(1), 163-172 e164. https://doi.org/10.1016/j.cub.2020.10.043

Le Merre, P., Esmaeili, V., Charriere, E., Galan, K., Salin, P. A., Petersen, C. C. H., & Crochet, S. (2018). Reward-Based Learning Drives Rapid Sensory Signals in Medial Prefrontal Cortex and Dorsal Hippocampus Necessary for Goal-Directed Behavior. *Neuron*, *97*(1), 83-91 e85. https://doi.org/10.1016/j.neuron.2017.11.031

Lee, K. H., Bhaker, R. S., Mysore, A., Parks, R. W., Birkett, P. B., & Woodruff, P. W. (2009). Time perception and its neuropsychological correlates in patients with schizophrenia and in healthy volunteers. *Psychiatry Res*, *166*(2-3), 174-183. https://doi.org/10.1016/j.psychres.2008.03.004

Makino, H., Ren, C., Liu, H., Kim, A. N., Kondapaneni, N., Liu, X., Kuzum, D., & Komiyama, T. (2017). Transformation of Cortex-wide Emergent Properties during Motor Learning. *Neuron*, *94*(4), 880-890 e888. https://doi.org/10.1016/j.neuron.2017.04.015

Mar, A. C., Walker, A. L., Theobald, D. E., Eagle, D. M., & Robbins, T. W. (2011). Dissociable effects of lesions to orbitofrontal cortex subregions on impulsive choice in the rat. *J Neurosci*, *31*(17), 6398-6404. https://doi.org/10.1523/JNEUROSCI.6620-10.2011

Marrero, K., Aruljothi, K., Zareian, B., Gao, C., Zhang, Z., & Zagha, E. (2022). Global, Low-Amplitude Cortical State Predicts Response Outcomes in a Selective Detection Task in Mice. *Cereb Cortex*, *32*(9), 2037-2053. https://doi.org/10.1093/cercor/bhab339

McBurney-Lin, J., Sun, Y., Tortorelli, L. S., Nguyen, Q. A. T., Haga-Yamanaka, S., & Yang, H. (2020). Bidirectional pharmacological perturbations of the noradrenergic system differentially affect tactile detection. *Neuropharmacology*, *174*, 108151. https://doi.org/10.1016/j.neuropharm.2020.108151

McClure, S. M., Berns, G. S., & Montague, P. R. (2003). Temporal Prediction Errors in a Passive Learning Task Activate Human Striatum. *Neuron*, *38*(2), 339-346. https://doi.org/10.1016/S0896-6273(03)00154-5

Meilleur, A., Foster, N. E. V., Coll, S. M., Brambati, S. M., & Hyde, K. L. (2020). Unisensory and multisensory temporal processing in autism and dyslexia: A systematic review and meta-analysis. *Neurosci Biobehav Rev*, *116*, 44-63. https://doi.org/10.1016/j.neubiorev.2020.06.013

Mendonça, A. G., Drugowitsch, J., Vicente, M. I., DeWitt, E. E. J., Pouget, A., & Mainen, Z. F. (2020). The impact of learning on perceptual decisions and its implication for speed-accuracy tradeoffs. *Nature Communications*, *11*(1), 2757. https://doi.org/10.1038/s41467-020-16196-7

Mobini, S., Body, S., Ho, M. Y., Bradshaw, C. M., Szabadi, E., Deakin, J. F., & Anderson, I. M. (2002). Effects of lesions of the orbitofrontal cortex on sensitivity to delayed and probabilistic reinforcement. *Psychopharmacology (Berl)*, *160*(3), 290-298. https://doi.org/10.1007/s00213-001-0983-0

Murakami, M., Shteingart, H., Loewenstein, Y., & Mainen, Z. F. (2017). Distinct Sources of Deterministic and Stochastic Components of Action Timing Decisions in Rodent Frontal Cortex. *Neuron*, *94*(4), 908-919 e907. https://doi.org/10.1016/j.neuron.2017.04.040

Namboodiri, V. M., Huertas, M. A., Monk, K. J., Shouval, H. Z., & Hussain Shuler, M. G. (2015). Visually cued action timing in the primary visual cortex. *Neuron*, *86*(1), 319-330. https://doi.org/10.1016/j.neuron.2015.02.043

Narayanan, N. S., Horst, N. K., & Laubach, M. (2006). Reversible inactivations of rat medial prefrontal cortex impair the ability to wait for a stimulus. *Neuroscience*, *139*(3), 865-876. https://doi.org/10.1016/j.neuroscience.2005.11.072

Narayanan, N. S., Land, B. B., Solder, J. E., Deisseroth, K., & DiLeone, R. J. (2012). Prefrontal D1 dopamine signaling is required for temporal control. *Proc Natl Acad Sci U S A*, *109*(50), 20726-20731. https://doi.org/10.1073/pnas.1211258109

Nobre, A. C., Correa, A., & Coull, J. T. (2007). The hazards of time. *Current Opinion in Neurobiology*, *17*(4), 465-470. https://doi.org/https://doi.org/10.1016/j.conb.2007.07.006

O'Doherty, J. P., Dayan, P., Friston, K., Critchley, H., & Dolan, R. J. (2003). Temporal Difference Models and Reward-Related Learning in the Human Brain. *Neuron*, *38*(2), 329-337. https://doi.org/10.1016/S0896-6273(03)00169-7

Pai, S., Erlich, J. C., Kopec, C., & Brody, C. D. (2011). Minimal impairment in a rat model of duration discrimination following excitotoxic lesions of primary auditory and prefrontal cortices. *Front Syst Neurosci*, *5*, 74. https://doi.org/10.3389/fnsys.2011.00074

Pardey, M. C., Homewood, J., Taylor, A., & Cornish, J. L. (2009). Re-evaluation of an animal model for ADHD using a free-operant choice task. *J Neurosci Methods*, *176*(2), 166-171. https://doi.org/10.1016/j.jneumeth.2008.09.009

Paton, J. J., & Buonomano, D. V. (2018). The Neural Basis of Timing: Distributed Mechanisms for Diverse Functions. *Neuron*, *98*(4), 687-705. https://doi.org/10.1016/j.neuron.2018.03.045

Peterson, B. S., Skudlarski, P., Gatenby, J. C., Zhang, H., Anderson, A. W., & Gore, J. C. (1999). An fMRI study of stroop word-color interference: evidence for cingulate subregions subserving multiple distributed attentional systems. *Biological Psychiatry*, *45*(10), 1237-1258. https://doi.org/https://doi.org/10.1016/S0006-3223(99)00056-6

Pisupati, S., Chartarifsky-Lynn, L., Khanal, A., & Churchland, A. K. (2021). Lapses in perceptual decisions reflect exploration. *Elife*, *10*. https://doi.org/10.7554/eLife.55490

Reinert, S., Hubener, M., Bonhoeffer, T., & Goltstein, P. M. (2021). Mouse prefrontal cortex represents learned rules for categorization. *Nature*, *593*(7859), 411-417. https://doi.org/10.1038/s41586-021-03452-z

Remmelink, E., Smit, A. B., Verhage, M., & Loos, M. (2016). Measuring discrimination- and reversal learning in mouse models within 4 days and without prior food deprivation. *Learning & Memory*, *23*(11), 660-667. http://learnmem.cshlp.org/content/23/11/660.abstract

Reyes, M. B., de Miranda, D. H., Tunes, G. C., Cravo, A. M., & Caetano, M. S. (2020). Rats can learn a temporal task in a single session. *Behav Processes*, *170*, 103986. https://doi.org/10.1016/j.beproc.2019.103986

Richter, S. H., & von Kortzfleisch, V. (2020). It is time for an empirically informed paradigm shift in animal research. *Nat Rev Neurosci*, *21*(11), 660. https://doi.org/10.1038/s41583-020-0369-0

Robbins, T. W., & Dalley, J. W. (2017). *Impulsivity, risky choice, and impulse control disorders: Animal models*. Elsevier Inc. https://doi.org/10.1016/B978-0-12-805308-9.00007-5

Roitman, J. D., & Shadlen, M. N. (2002). Response of Neurons in the Lateral Intraparietal Area during a Combined Visual Discrimination Reaction Time Task. *The Journal of Neuroscience*, *22*(21), 9475-9489. https://doi.org/10.1523/jneurosci.22-21-09475.2002

Romo, R., & Schultz, W. (1990). Dopamine neurons of the monkey midbrain: contingencies of responses to active touch during self-initiated arm movements. *Journal of Neurophysiology*, *63*(3), 592-606. https://doi.org/10.1152/jn.1990.63.3.592

Roy, N. A., Bak, J. H., International Brain, L., Akrami, A., Brody, C. D., & Pillow, J. W. (2021). Extracting the dynamics of behavior in sensory decision-making experiments. *Neuron*. https://doi.org/10.1016/j.neuron.2020.12.004

Rubia, K., Halari, R., Christakou, A., & Taylor, E. (2009). Impulsiveness as a timing disturbance: neurocognitive abnormalities in attention-deficit hyperactivity disorder during temporal processes and normalization with methylphenidate. *Philos Trans R Soc Lond B Biol Sci*, *364*(1525), 1919-1931. https://doi.org/10.1098/rstb.2009.0014

Rudebeck, P. H., & Murray, E. A. (2008). Amygdala and orbitofrontal cortex lesions differentially influence choices during object reversal learning. *J Neurosci*, *28*(33), 8338-8343. https://doi.org/10.1523/JNEUROSCI.2272-08.2008

Ruff, D. A., & Cohen, M. R. (2019). Simultaneous multi-area recordings suggest that attention improves performance by reshaping stimulus representations. *Nat Neurosci*, *22*(10), 1669-1676. https://doi.org/10.1038/s41593-019-0477-1

Schoenbaum, G., & Roesch, M. (2005). Orbitofrontal cortex, associative learning, and expectancies. *Neuron*, *47*(5), 633-636. https://doi.org/10.1016/j.neuron.2005.07.018

Schultz, W., Apicella, P., & Ljungberg, T. (1993). Responses of monkey dopamine neurons to reward and conditioned stimuli during successive steps of learning a delayed response task. *The Journal of Neuroscience*, *13*(3), 900-913. https://doi.org/10.1523/jneurosci.13-03-00900.1993

Shuler, M. G., & Bear, M. F. (2006). Reward timing in the primary visual cortex. *Science*, *311*(5767), 1606-1609. https://doi.org/10.1126/science.1123513

Smits-Bandstra, S., & De Nil, L. F. (2007). Sequence skill learning in persons who stutter: implications for cortico-striato-thalamo-cortical dysfunction. *J Fluency Disord*, *32*(4), 251-278. https://doi.org/10.1016/j.jfludis.2007.06.001

Song, Y.-H., Hwang, Y.-S., Kim, K., Lee, H.-R., Kim, J.-H., Maclachlan, C., Dubois, A., Jung, M. W., Petersen, C. C. H., Knott, G., Lee, S.-H., & Lee, S.-H. (2020). Somatostatin enhances visual processing and perception by suppressing excitatory inputs to parvalbumin-positive interneurons in V1. *Science Advances*, *6*(17), eaaz0517. https://doi.org/doi:10.1126/sciadv.aaz0517

Toplak, M. E., Dockstader, C., & Tannock, R. (2006). Temporal information processing in ADHD: findings to date and new methods. *J Neurosci Methods*, *151*(1), 15-29. https://doi.org/10.1016/j.jneumeth.2005.09.018

van Maanen, L., Grasman, R. P., Forstmann, B. U., & Wagenmakers, E. J. (2012). Pieron's Law and Optimal Behavior in Perceptual Decision-Making. *Front Neurosci*, *5*, 143. https://doi.org/10.3389/fnins.2011.00143

Winstanley, C. A., Theobald, D. E., Dalley, J. W., Glennon, J. C., & Robbins, T. W. (2004). 5-HT2A and 5-HT2C receptor antagonists have opposing effects on a measure of impulsivity: interactions with global 5-HT depletion. *Psychopharmacology (Berl)*, *176*(3-4), 376-385. https://doi.org/10.1007/s00213-004-1884-9

Womelsdorf, T., & Fries, P. (2007). The role of neuronal synchronization in selective attention. *Curr Opin Neurobiol*, *17*(2), 154-160. https://doi.org/10.1016/j.conb.2007.02.002

Xiong, Q., Znamenskiy, P., & Zador, A. M. (2015). Selective corticostriatal plasticity during acquisition of an auditory discrimination task. *Nature*, *521*(7552), 348-351. https://doi.org/10.1038/nature14225

Yang, G. R., Joglekar, M. R., Song, H. F., Newsome, W. T., & Wang, X. J. (2019). Task representations in neural networks trained to perform many cognitive tasks. *Nat Neurosci*, *22*(2), 297-306. https://doi.org/10.1038/s41593-018-0310-2

Zareian, B., Lam, A., & Zagha, E. (2022). Dorsolateral striatum, not motor cortex, is a bottleneck for responding to task-relevant stimuli in a learned whisker detection task in mice. *bioRxiv*, 2022.2003.2003.482906. https://doi.org/10.1101/2022.03.03.482906

Zareian, B., Zhang, Z., & Zagha, E. (2021). Cortical Localization of the Sensory-Motor Transformation in a Whisker Detection Task in Mice. *eNeuro*, ENEURO.0004-0021. https://doi.org/10.1523/eneuro.0004-21.2021

Zariwala, Hatim A., Kepecs, A., Uchida, N., Hirokawa, J., & Mainen, Zachary F. (2013). The Limits of Deliberation in a Perceptual Decision Task. *Neuron*, *78*(2), 339-351. https://doi.org/https://doi.org/10.1016/j.neuron.2013.02.010

Zhang, Z., & Zagha, E. (2022). Frontal Cortex Gates Distractor Stimulus Encoding in Sensory Cortex. *bioRxiv*, 2022.2003.2031.486430. https://doi.org/10.1101/2022.03.31.486430

Zhao, S., Ting, J. T., Atallah, H. E., Qiu, L., Tan, J., Gloss, B., Augustine, G. J., Deisseroth, K., Luo, M., Graybiel, A. M., & Feng, G. (2011). Cell type-specific channelrhodopsin-2 transgenic mice for optogenetic dissection of neural circuitry function. *Nat Methods*, *8*(9), 745-752. https://doi.org/10.1038/nmeth.1668